

DEGREE PROJECT



Journal Bearing Friction Optimization

Szeréna - Krisztina Ujvári

Mechanical Engineering, masters level
2016

Luleå University of Technology
Department of Engineering Sciences and Mathematics



Acknowledgments

I would like to thank Luleå University of Technology for the opportunity to study as one of the *2nd* generation Erasmus Mundus TRIBOS students. Being part of the small group who finished their last year in the North was not only a great experience but also an unique adventure.

I would like to express my great appreciation to my supervisor Prof. Braham Prakash, who helped me throughout the year, by not only giving professional guidance, but moral encouragement too. I am glad that I could work under his supervision and to learn a lot about how to implement an experimental study.
I would also like to say thanks to Prof. Roland Larsson, my second supervisor, for his assistance and guidance with the difficulties encountered along the way.

I would like to offer my special thanks to Dr. Jens Johansson, who not only helped me with the development of the test rig, but also each time I had difficulties during the experimental work.

Accomplishing my thesis work, would not be possible without the support of Sabine Fleiss and Fredrik Strömstedt, my two supervisors from Volvo Car Corporation. They not only invested their time and guidance throughout the project, but also gave a lot of help and technical support. Working with them was a valuable experience for me.

I am grateful for the help, encouragement and kindness of several people, from Machine Elements division and the ones working in Tribolab. Also special thanks to the LTU Workshop for making it possible to manufacture the shaft samples in time.

I would like to acknowledge my dear colleagues for their help and for the great time we spent together. Special thanks to my colleague Ding Liang, for his help, patience and collaboration. Working with him was a great experience.

Last but not least, I want to say thanks to all the lovely people I met at LTU, to my friends, for their support, the many hours of laughter and for this memorable year.

Abstract

Engine downsizing, improving fuel efficiency while satisfying the environmental legislations are one of the main driving forces in developing new solutions for passenger cars.

Engine main bearings, are journal bearings which support the crankshaft and operate principally in full film lubrication. Defining the optimum design parameters of the bearings which can provide low friction and high durability for automobiles represents a multi-variable problem.

Being the supporters of the main shaft driven by the internal combustion engine, main bearings are subjected to strenuous operating conditions. These include high loads and pressures amongst others. The trend in lubricant selection for these components is shifting towards choosing engine oils with lower viscosity to further reduce fuel consumption. Simultaneously with the shift in oil, new solutions for controlling the geometry and the topography on the micro-scale are becoming available.

Three main bearing top layers plated on a conventional aluminum alloy containing tin and silicon were selected for the study. The top layers, one bismuth based and two newly developed polymer based, were investigated for their frictional and wear performance.

In order to study experimentally the influence of different design parameters on bearing performance a test rig and a methodology was developed.

The selected engine main bearings were tested in lubricated condition with two oils having different viscosity. Pre - and post test analysis of the shaft surface roughness was performed using white light interferometry. The wear performance of the bearings was measured both as mass loss and surface topography.

The results suggest that the developed test rig can be used to simulate close to running condition testing. The measurement method and set up shows good consistency at a load of 2000 N, but indicates inconsistency in set up at 500 N.

It is found that the newly developed engine main bearing top layers have promising frictional and wear performance, providing a reduction in friction by up to 20%.

Contents

1	Introduction	6
1.1	Hydrodynamic journal bearings	7
1.2	Crankshaft bearing system	9
1.3	Tribology and optimization of engine main bearings	11
1.3.1	Tribology of main bearings - Lubrication	11
1.3.2	Bearing materials	13
1.4	Solutions for journal bearing friction optimization	16
1.4.1	New, lead free bearings	16
1.4.2	Surface finish solutions for improving the bearing- crankshaft contact	17
1.4.3	Engine friction testing	18
2	Materials and Experiments	22
2.1	Specimens and materials	22
2.2	Test parameters	25
2.3	Testing procedure	26
2.4	Specimen characterization and analysis	28
3	Results and Discussion	29
3.1	Design of the test rig	29
3.1.1	Developed test methodology	32
3.2	Analysis of experimental data	34
3.2.1	Friction Performance	34
3.2.2	Performance of bearing top layers	37
3.2.3	Effect of lubricant viscosity - polymer top layer MoS ₂ + PAI	40
3.3	Running-in behavior and Wear performance	41
3.3.1	Effect of shaft surface roughness	41
3.3.2	Bearing top layer wear behavior	41
3.4	Surface Analysis	44
3.4.1	Surface roughness measurements with 3D optical microscope .	44
3.4.2	Surface topography images	49
3.5	Summary and Discussion	52
4	Conclusions	59

Nomenclature

μ	Viscosity
ϕ	Attitude Angle: Angle from -Y axis to Line of Centers
C_b	Radial Clearance of the Bearing: $R_b - R_j$
e	Eccentricity - the distance between the center of the bearing and the center of the shaft
e/C_b	Eccentricity Ratio - if zero, shaft is centered; if 1 then shaft touches bearing
h	Radial clearance as a function of the angular position where the clearance is measured
h_{min}	Minimum oil film clearance
L	Bearing length
n	Rotational speed
R_b	Radius of the Bearing
R_j	Radius of Journal
W	Load

Chapter 1

Introduction

Overcoming the resistance to motion has been a great challenge for humankind since the first machines have been built. Early on, friction, wear and lubrication was recognized to have a crucial influence on the efficiency and durability of various machinery. Improvements, and a great amount of scientific research established the foundation for the scientific field called tribology [1, 2].

One of todays biggest challenges is to produce energy efficient vehicles and machines, not only for economic, but also for environmental reasons. Legislative demands for finding environmental friendly solutions and the urge to reduce CO_2 emissions due to climate change [3], represent some of the the main driving forces for many big companies.

Particularly in the automotive industry these tasks require urgent and effective solutions. Due to engine downsizing and high expectations in performance, this field is experiencing great advancements.

The introduced legislations concerning the environmental impact of internal combustion engines (ICE) affect the manufacture of some of the essential components. For example, in case of connecting rod and engine main bearings the legislations require the elimination of lead from the bearings and it's replacement with less toxic alternatives. Furthermore, it demands the development of bearings that show good performance when they are lubricated with a less viscous engine oil in order to reduce the power losses which result from the oil pump and the engine. Moreover, it also compels manufacturers to produce bearings with reduced friction [4]. Recent research provides numerous studies on the energy use and friction losses in automotive vehicles, offering solutions for reducing friction by a series of performance optimization techniques [5].

A study from 2012 [6] reported that in passenger cars, less than one-third (21.5%) of the fuel energy is used to move the car. The direct frictional losses, excluding the breaking losses, add up to 28% of the total fuel energy.

It was found that applying the most advanced tribological solutions available today in all existing tribocontacts of passenger cars, frictional losses can be reduced by 61% in the next 20 years.

The aim of this thesis work was to investigate and define the optimal bearing parameters for the crankshaft main bearing system and rank different bearing top layers in terms of their frictional and wear performance. The first part of the study however deals with the development of a test rig and a methodology, that can provide representative results.

1.1 Hydrodynamic journal bearings

Engine main bearings are hydrodynamic journal bearings which are designed to operate in fully lubricated conditions. One of the main advantages of journal bearings is that the lubricant film prevents localized overloading by providing a distribution of the applied force over a relatively wide area (Fig. 1.1). At zero speed the loaded

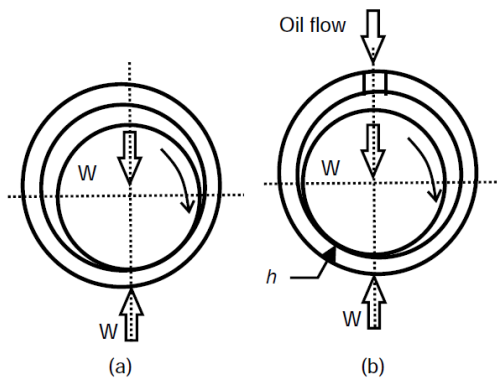


Figure 1.1: Hydrodynamic journal bearing - pressure build up [7].

journal rests on the bearing at its bottom center, and the two surfaces are in contact. At startup, when there is less oil, the journal climbs up on the right side of the bearing. As soon as the rotational speed increases, more oil is supplied to the gap between the journal and the bearing. The developed converging wedge forces the journal to lift and move to the left, where a thin oil film that separates the two surfaces is formed.

Therefore, the moving surface drags the lubricant, into the converging gap and the lubricant carries the applied load. As the space available in this gap decreases, the fluid develops a pressure gradient, or pressure hill (Figure 1.2). At the exit of the contact, there is in turn a diverging gap where the pressure drops to the cavitation pressure which is close to the atmospheric pressure. The developed pressure distribution together with the hydrodynamic friction force will act with an equal but opposing force to the load.

The pressure distribution is a function of load, speed, clearance and the lubricant viscosity. The location where the pressure is at maximum represents a critical region for the bearing. This is where, a decrease in oil film thickness can cause surface-to-surface contact, leading to increase in friction and even adhesive or abrasive wear [7].

Journal bearings have the advantages of providing damping which is required in order to pass through the critical speed, where instabilities and vibration are likely to occur during operation.

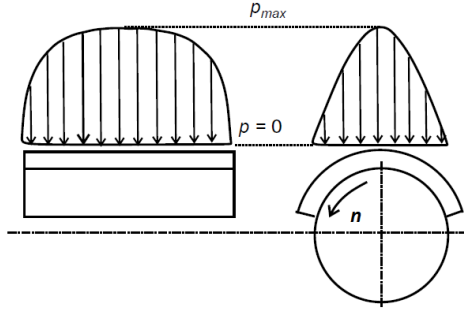


Figure 1.2: The pressure distribution in the bearing resulting from hydrodynamic operation. [7].

The position of the journal in the diametrical clearance (C_b), the gap between the journal and the bearing inner diameter, defines the eccentricity. During operation when the eccentricity is too high there is a risk of surface-to-surface contact and the higher dynamic loads acting on the lower bearing shell can cause premature fatigue. If the eccentricity is relatively low, i.e. when the journal is almost centered, instability issues can typically arise. Therefore, the eccentricity which is a function of both speed and load which characterizes the stability of the bearing.

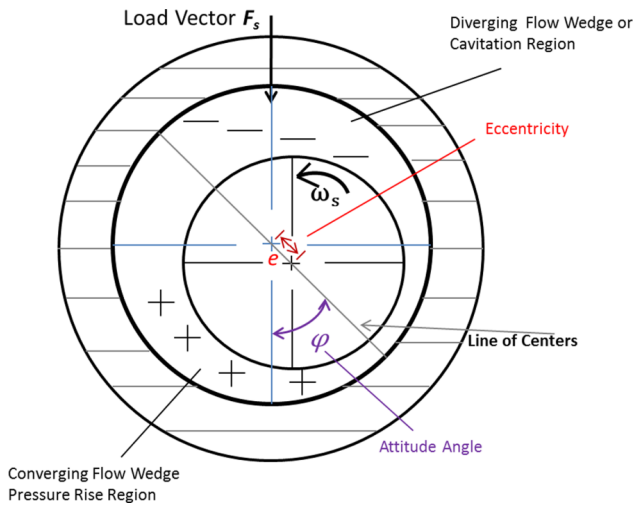


Figure 1.3: Hydrodynamic journal bearing [8]. Note that the image shows an exaggerated film thickness.

Looking at Figure 1.3 can give a clearer picture about the journal's location during running condition. The attitude angle between the vertical axis in the load direction and the line of centers is also a function of speed. As the rotational speed increases, the locus of the journal's center line will climb closer to the center following a curve. Combining the effect of speed and load, the result is the following: at low speeds and high load the eccentricity ratio e/C_b is close to unity, while at high speed, the eccentricity is close to zero.

Therefore, when choosing the optimal design for a journal bearing, clearance becomes one of the important factors that has a great influence on the performance of the bearing.

Although, the selected clearance value plays a main role in determining the film thickness there are other factors that needs to be taken into account. The surface topography and the roughness of the two mating parts also play a crucial role in the efficient lubrication of the contact. Precise design and detailed analysis of the mating surfaces is needed in order to achieve increased bearing life and performance. [9–11].

1.2 Crankshaft bearing system

In the IC engine, the main bearings support the crankshaft and connecting rod bearings provide a low friction relative motion (rotation) between connecting rod and crankshaft. Both are sleeve type sliding bearings, called half bearings. Each bearing pair surrounds a crankshaft journal.

Main bearings are mounted to the engine block with a cap or ladder frame and support the crankshaft. They are designed to allow rotation under inertia forces and oscillating forces transmitted by the connecting rods. The main bearing consists of a lower part which supports the load, and an upper part. The upper part has a hole and a groove to supply the lubricating oil [12, 13]. Connecting rod bearings are mounted in the big end of the connecting rod. For a clearer picture Figure 1.4 presents the location of the bearings.

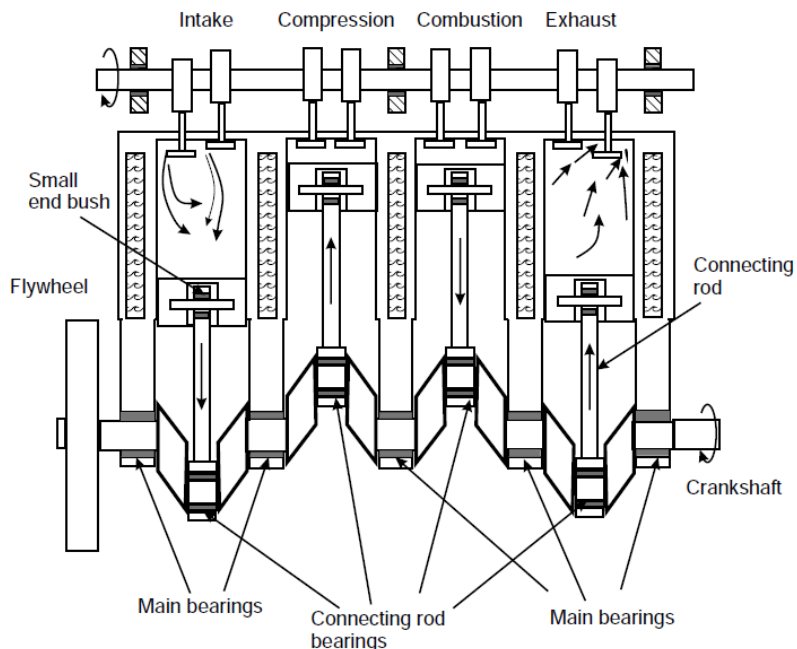


Figure 1.4: Typical engine block, pointing to the location of main bearings [7].

Table 1.1: Conditions in an automobile engine bearing [12]

Minimum lubricant film thickness	$1 \mu m$
Maximum shear rate (up to)	10^8 s^{-1}
Maximum bearing temperature	$120\text{--}150^\circ C$
Specific loading (up to)	60 MPa
Maximum film pressure	250 MPa
Lubricant dynamic viscosity	2.5^{10} Pas
Power loss per bearing high speed	0.25 kW
Flow rate per bearing (typically)	0.015 l/s

Continuous lubricant supply is maintained by the engine's lubrication system and is carried out by channels in the engine block. The lubricant film thickness in engine bearings is in the order of few micrometers. The absence of constant and sufficient supply of lubricant means improper cooling of the bearing surface that leads to severe wear and eventually seizure.

Both the main bearings and the connecting rod bearings run in different lubrication regimes depending on the operating conditions. Subjected to the loads generated by combustion and the reciprocating motion of the pistons, bearings have to work under very demanding conditions. The forces transmitted by the connecting rods from the pistons to the crankshaft are so high that they will result in a significant bending of the crankshaft. This bending will cause a misalignment of the crankshaft and will lead to edge loading on the the bearings [14]. To overcome the problem of small deviations in crankshaft or bearing diameter, typically the main bearings provided by the automotive industry come in different color grades, denoting their thickness values [15, 16].

The science behind the main bearing technology is evolving every year to suit the demanding requirements from the IC engines. Table 1.1 summarizes some of the important average conditions existing in automobile engine bearings. The presented data relates to a modern four-cylinder, four-stroke, gasoline engine. [12].

1.3 Tribology and optimization of engine main bearings

Three distinctive categories can be identified where improvements can potentially increase the overall bearing performance. These are the following: geometry, material & lubricant selection and environmental factors.

In order to achieve the required performance and meet the regulations, all three need to be taken into consideration and designed with caution to form an optimized system. The following sections are aiming to provide a brief overview on the factors that influence bearing performance, with focus on tribological properties, material selection and surface characteristics.

1.3.1 Tribology of main bearings - Lubrication

Even though main bearings are designed to operate in hydrodynamic conditions, it has to be taken into account that at start-up and shut down there will be a contact between the mating surfaces leading to their operation in mixed / boundary lubrication and increased friction and wear.

The friction losses under hydrodynamic conditions are caused by the viscous shearing of the lubricant. When friction increases a higher torque is required to rotate the moving elements, leading to increase in power consumption. Therefore, viscosity is one the first factors to take into account when estimating the frictional losses. Moreover, viscosity changes with temperature rise and the variation can be highly non-linear. Frictional losses in the journal bearing are a function of viscosity, load, and speed.

Lubricated friction is characterized by the presence of a thin film of the pressurized lubricant between the surfaces of the bearing and the journal. The ratio of the squeeze film thickness to the surface roughness indicates the type of the lubrication regime.

Separating the lubrication regimes according to the film thickness ratio is used as a design concept for lubricated contacts. Since the film thickness ratio is characterizing the occurrence of surface interaction and is directly related to the surface topography of the contact it can be used to represent the performance and durability of lubricated components. The typical curve that is used to represent in which regime the bearing is operating is shown on Figure 1.5.

The Stribeck diagram represents all three lubrication regimes. The performance factor in each regime is given by the coefficient of friction which is a function of the non-dimensional Hersey number (H_n):

$$H_n = \eta \times N/p_{av} \quad (1.1)$$

where η stands for the dynamic viscosity, N is the rotational speed and p_{av} denotes the average bearing pressure . According to the Stribeck curve the highest coefficient of friction can be found in boundary lubrication regime, leading to temperature rise and wear. In the mixed lubrication regime, when the oil film starts to form and the

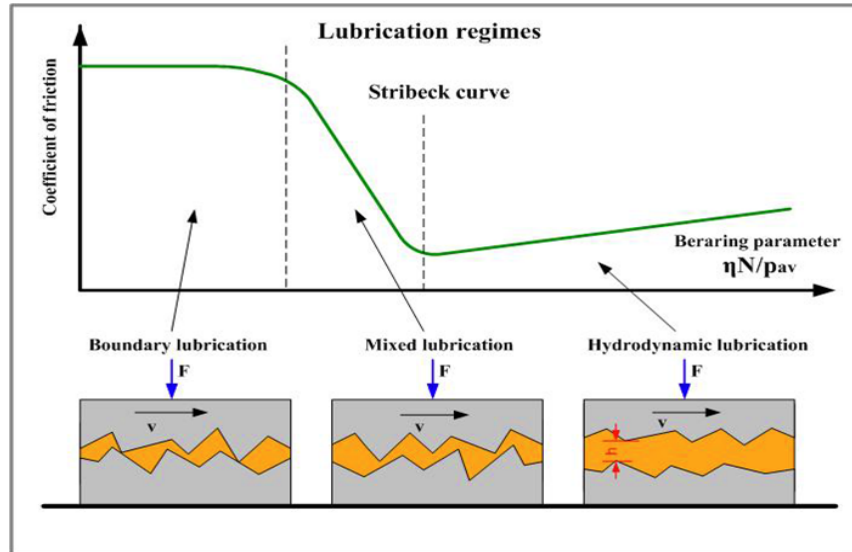


Figure 1.5: Lubrication regimes represented by the Stribeck curve [10]

contact between the surfaces starts to decrease, causes a steep fall in the friction coefficient. Temperature rise due to friction in the mixed regime also causes a drop in lubricant viscosity. This leads to an increase of the bearing parameter. However a small change in the bearing parameter, can cause a huge increase in the friction coefficient, therefore this regime is the most unstable.

If the rotational speed is increased, the bearing can pass to the hydrodynamic, full film lubrication, where the coefficient of friction is the smallest. The Hersey number will increase due to temperature rise, causing the viscosity to decrease, resulting in a drop in the value of the friction coefficient. Consequently, the temperature will drop. Due to this counterbalance, the hydrodynamic regime becomes the most stable.

Relevance of lubrication regimes on journal bearing design

When the film thickness h is lower than the surface roughness there will be a constant contact between the surfaces at high surface points. The boundary lubrication regime is the most critical and undesirable lubrication regime, since it is characterized by high friction accompanied by increased wear and possibility of seizure of the bearing and journal. Severe engine bearing failures usually happen during operation in boundary lubrication.

Compatibility of the bearing with the shaft material plays a crucial role in ensuring that the tribological system functions optimally. If a too soft material is selected for the bearing, heavy running-in wear of the bearing and ploughing of the shaft surface asperities on the softer bearing surfaces would occur.

The selected material for both the bearing and shaft have to be able to absorb and conduct away the heat generated without excessive temperature rise. The shafts are nitrided or induction hardened and have a hardness around 56 HRC. The hardness of the bearing material is typically in the range of 25HV for white metal bearings, 45–100HV for lead-based half bearings, while aluminum-based materials are typi-

cally in the range 30–60HV [7].

Furthermore, it is essential to choose and manufacture the surface finish of the shaft carefully, as the soft bearing material can duplicate the roughness of the shaft it mates with.

In the mixed lubrication regime local fluid film lubrication and intermittent contact between the micro-asperities are expected.

Lead-based top layers have been popularly used to reduce friction, but today new materials such as molybdenum disulfide are becoming a more suitable alternative [10]. Since modifying and controlling the surface topography with high precision is possible nowadays, bearing surfaces are designed to have small holes for oil retention and oil flow at the same time, produced by boring techniques, in order to provide mixed lubrication condition and avoid operation in boundary lubrication. This is due to the oil collecting in the pores created through this manufacturing technique.

In the hydrodynamic regime the load is fully supported by the lubricant, therefore there is no wear and only the hydrodynamic friction is responsible for the energy losses.

Because engine main bearings are designed to work in hydrodynamic lubrication regime, choosing an engine oil with the optimal viscosity is crucial in reducing the frictional losses. The rotation of the shaft causes shearing of the oil film between it and the stationary bearing surface. The shearing action creates a stress field in the lubricant film, whilst the shear rate will be defined by the relative velocity between the surfaces. Since the dynamic viscosity is the ratio of the shear stress to the shear rate, high viscosity lubricants increase the shear stress, while low viscosity lubricants increase the shear rate due to a smaller minimum film thickness.

A great deal of research was dedicated to find the best combinations of materials and lubricants that would give the lowest coefficient of friction [9, 10, 17].

1.3.2 Bearing materials

The selection of bearing materials which can ensure durable and energy efficient operation represents a complex and non-trivial task. The low friction materials used for main bearings also require high performance in terms of seizure resistance, running-in and wear resistance [18]. Moreover, the durable operation of an engine bearing is ensured if the combined materials provide both high strength and are soft enough in order to allow conformability and embedability. This compromise between material properties can be achieved by a bearing with composite structure. The composite structure can be of two types: layered, i.e. soft overlay on a strong lining, or particulate, i.e. small particles of a strong material distributed in a relatively soft matrix.

Main bearings are designed as two-material or three-material bearings. Bi-metal bearings (Figure 1.7) typically consist of a functional surface layer on a steel backing. They are used engines under low or medium loads. Three-metal bearings are composed of a slide layer, a barrier layer and a bronze or copper based bearing

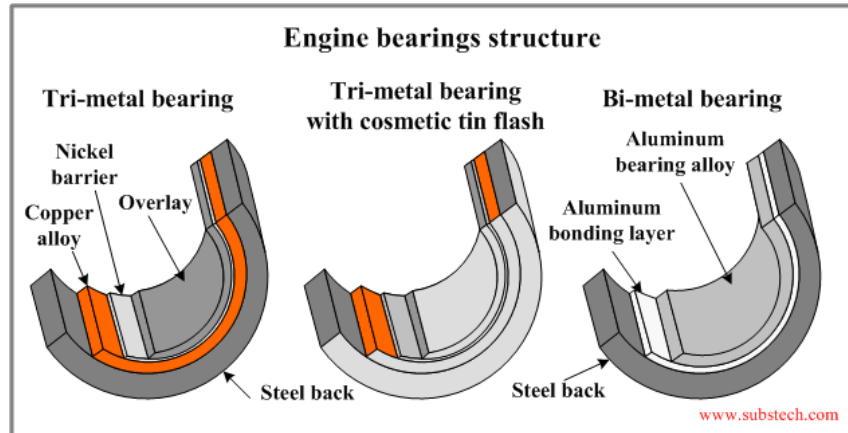


Figure 1.6: Engine bearing types. [11]

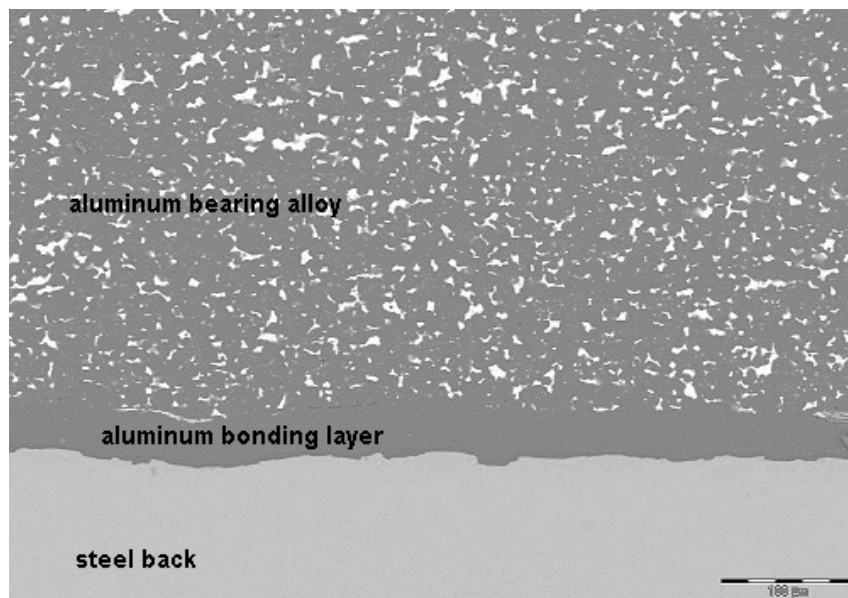


Figure 1.7: Micro-structure of a bimetal bearing [11]

layer, cast or sintered to the steel backing, and are usually used in engines exposed to higher loads.

The typical structure of engine main bearings is presented on Figure 1.6. The function of the different layers is discussed below.

The **steel backing** supports the bearing structure and provides its stiffness making it resistant under demanding conditions of increased temperature and high loads.

The **intermediate layer** is the layer placed between the steel back and the overlay. This layer is designed to have moderate or low friction properties, but high fatigue strength providing durability to the bearing.

The intermediate layer is usually made of copper alloys such as CuPbSn (leaded bronzes), CuAl (aluminum bronzes) or CuBiSn. They are applied on the steel back surface by casting or sintering processes.

Aluminum alloys containing tin and silicon are used also as intermediate layer materials. These materials are bonded to the steel back by the cold-rolling bonding method. The thickness of the intermediate layers is varies between 0.2 and 0.4 mm.

Between the intermediate layer and the overlay a **nickel diffusion barrier** is deposited in order to prevent diffusion of tin from the overlay into the intermediate material. The reason for using such a layer is to prevent the formation of brittle inter-metallic compounds which can have a negative effect on the adhesion strength of the overlay to the intermediate layer.

An **overlay** is the top layer made of a soft material (i.e. PbSnCu, SnCu, PbIn, or either graphite or molybdenum disulfide added to a polymer-based materials) with very good low-friction properties, seizure resistance, compatibility, conformability and embeddability. Their thickness is usually within the range of 12–25 μm . Applying the overlays at a certain thickness is needed to ensure good fatigue strength which is inversely proportional with the overlay thickness. Their use becomes vital in conditions of engine start and shutdown [7].

In conclusion, for selection of main bearing materials, the general rules that need to be taken into account are the following. From a chemical point of view, the alloy has to be corrosion resistant and non toxic; while from a mechanical point of view, the alloy must have high resistance to withstand the high pressures in the engine, but its hardness must be low enough not to damage the shaft [19].

In the past, the most suitable combination for journal bearing inner layers were found to be lead-, tin-, copper- and aluminum-based materials. From the point of view of their performance, lead- and tin-based materials have the best sliding properties but show lower strength compared to the copper based materials. Although, having one of the most desired properties, the usage of lead is very limited nowadays and soon needs to be eliminated from engine components.

1.4 Solutions for journal bearing friction optimization

1.4.1 New, lead free bearings

As of late urgency to find lead-free solutions, aluminum bearing materials have become the most promising inner layer alternatives.

Aluminum bearing materials offer a good combination of relatively high strength and good sliding properties, and are capable of operating under demanding conditions without the need for overlay coatings. The absence of the overlay reduces the manufacturing cost of the half-bearing which makes it the most suitable bearing material for many engineering applications [18].

Aluminum-Tin based bearing materials

Aluminum-based alloys with the addition of tin or silicon have enhanced tribological and mechanical properties and are used by every major bearing manufacturer.

In general, Al-Sn alloys have good low-friction characteristics but due to the soft nature of tin, they are inefficient in supporting heavy loads. In order to enhance the load carrying capacity hard particles can be added to the alloy. It was found that the wear resistance of the Al-Sn-Cu-Si alloy is considerably higher than that of an Al-Sn-Cu or Al-Sn-Cu-Ni alloy due to the existence of hard Si particles. Studies showed [20] that the wear rate of the Al-Sn-Si alloys decreases with increasing Sn and Si contents, and the friction factor decreases slightly with an increase in Sn content but increase in Si content introduces only a slight variation.

Moreover, the Al-Sn-Si alloys exhibit excellent seizure resistance due to the presence of a hard silicon phase [21, 22].

Bismuth containing bearing top layers

Known to have similar properties to lead, bismuth was found to give surprisingly good physical properties to engine bearings. Either when alloyed to powder metal bronze in a low amount [23] or plated as an overlay on the top of the lining alloy [24], the bearings exhibited equal or better resistance compared to traditional lead containing engine bearings. According to a paper published in 2004 [23], the lead-free bearing with a powder metal lining composed of copper, tin, phosphorus and up to 5% bismuth by weight, demonstrated improved wear and seizure properties. It has been found that during operation a certain amount of the tin, which was initially fully dissolved in the uniform copper-tin matrix, migrates to the bearing surface. The formed tin rich layer serves as a solid-lubricant and improves the wear and seizure resistance of the bearing. The study attributes the mobilization of tin to the bearing surface due to the presence of bismuth in the matrix, since it has not been found on the surface of copper-tin-lead bearings.

When Bi (first layer) together with silver (second layer) was used as overlay on top of the lining, it was found to provide improved performance in preventing seizure. The improved performance was attributed to its lipophilic property, the existence of the microscopic grooves on the surface which can retain the lubricant by the capillary phenomenon. The paper also reported that the top Bi overlay was worn

out during wear tests exposing the silver layer. This however did not decrease the seizure resistance of the bearing. [24].

Polymer based coatings

Polymer based top layers have been applied to serve as running-in layers and lately as permanent layers as well. Polyamide-imide (PAI) is a widely used amorphous thermoplastic. The PAI base resin is known to provide superior mechanical strength at high temperatures and also shows great chemical resistance. It shows high resistance against diesel fuel and also engine oil [25]. In order to control the friction and provide good compatibility, solid lubricant fillers, such as molybdenum-disulphide and graphite are added to the polymeric matrix.

Functioning as permanent layer, this composite material can reduce friction at start-up or in cases when the lubricant film breaks down.

A paper from 2014 reported on an experimental study of a bearing with MoS_2

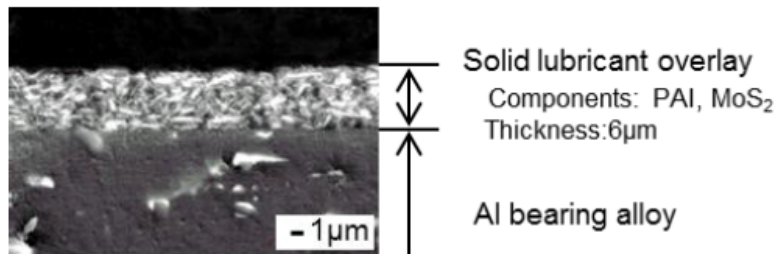


Figure 1.8: The cross-sectional view of the PAI + MoS_2 top layer [26].

solid lubricant and polyamide-imide resin coated overlay. The experimental results compared to a bimetal aluminium bearing without overlay showed a 40% reduction in friction coefficient and 65% less bearing wear, in close to boundary lubrication conditions [26].

Besides molybdenum-dioxide and graphite, silicon carbide also can be added as a filler to the polymer matrix. Adding silicon carbide particles can improve the thermal conductivity of the overlay without the risk of oxidation in contrast with metallic fillers. They also have the advantage of being lighter than metals and also inexpensive. Incorporating silicon carbide as a filler material in the polymer based bearing overlay is expected to improve the wear properties of the surface [27].

1.4.2 Surface finish solutions for improving the bearing-crankshaft contact

There are many surface roughness parameters for characterizing the surface either in two-dimension or three-dimension. Among all, the R_a is the most universally used, however such a single roughness parameter is not enough to describe functional properties like friction and lubrication. For example, in the investigations made by Lundberg et al. [28] the R_{max} and R_t were found to be the most significant

surface roughness parameters with regard to influence on lubrication.

The investigation made about the effects of the different surface topographies and surface finish techniques is in great interest of the automotive industries too. Modifying the surface of the crankshaft or the bearings in a controlled way, could lead to significant improvements in fuel efficiency.

A study [29] made on the effect of surface topography, analyzed the correlation between the surface roughness and frictional behavior and interpreted the results comparing Stribeck diagrams. Their findings showed improved frictional performance on post-treated ground surfaces resulting in a fine finish.

Singh et al. [30] conducted a study on the role of three-dimensional surface topographic characteristics of four precision finished surfaces (Ground, Hard Turned, Honed, and Isotropic) commonly used in the bearing industry. In their experiments they investigated the effect of surface type, sliding speed, and normal contact load on the coefficient of friction. Based on a detailed 3-D surface characterization, it was found that the amplitude parameter S_q (rms deviation of surface), spatial parameters S_{ds} (density of summits) and Std (texture direction) play an important role in determining the frictional behavior of the studied surfaces.

In a recent study [31] tribometric investigations on different shaft materials with varied surface conditions were conducted in order to investigate the bearing-shaft contact under start-stop motion. Forged steel and cast iron shaft materials were sliding against an Al based bearing alloy. They reported that the performance of forged steel depends on the overall roughness of the surface, whereas the tribological performance of cast iron is mainly determined through its microstructure. Their results prove the significance of optimized surface finishing of forged steel and cast iron shaft materials in order to minimize wear and friction in journal bearing systems.

1.4.3 Engine friction testing

Even with today's technology and rapid need to develop new materials, the testing and screening of engine components in lubricated condition is a difficult task. Engine friction testing methods exist on a wide range of scales from small test samples to test rigs, capable of simulating real-fired engine conditions for the full-sized components.

The true challenge is to develop and conduct such tests that can isolate the frictional performance of different components, such as main bearings, which are buried inside the engine.

Recently some studies used motored rigs instead of fired engines, aiming to isolate frictional behavior on subsystems. However, an issue requiring investigation is: how close to reality can these motored rigs simulate the operating conditions in the engine. A study made by Murti et al. [32] on a piston-assembly, evaluates the issues that arise in case these type of test rigs are used in order to simulate lubricant interactions with the coated surfaces.

Therefore, the development of new methods using motored test rigs is in the interest of many automotive companies. It enables engineers to test real life components at reduced costs, close to engine operating conditions. The future challenge is to evaluate and interpret the measured friction values within the tested conditions, and correlate them with real life conditions.

Summary

After a brief review of related literature it is undeniable that the changes in IC engines are occurring fast, as technology moves forward in the direction of high efficiency and lower emission vehicles.

The development of new bearing materials that can provide friction and wear reduction, stays in focus of many automotive companies. One of their big goals is to optimize the tribological system, using new low viscosity lubricants, lead-free bearing materials with functional overlays and well designed surfaces on the micro-scale. The main findings of this literature review can be summarized as follows:

- Bronze trimetal bearings are being replaced by aluminium-bimetal alternatives, aluminum-tin-silicon materials with minor additives, are one of the most promising in terms of friction and wear reduction, showing also excellent seizure resistance.
- The lead-based electrodeposited overlays which have dominated the bearing top layer solutions, have been replaced by tin-based overlays. Besides tin, another lead-free electrodeposited coatings that have been recently introduced, is a bismuth based overlay with a silver intermediate layer. It was found that the Bi-based overlay can provide improved seizure performance even after the top layer is worn out.
- Polymer-based coatings are also finding their way up, in the list of the promising friction reducing solutions. Since they are still newcomers to the field of hydrodynamic journal bearings, investigating their performance is of great interest.
- The polyamideimide (PAI) resin with additions of molybdenum disulfide (MoS₂), silicon-carbide (SiC) or graphite proved to be suitable to replace electrodeposited or sputtered overlays.
- The use of lubricants, with reduced viscosity offers promising results in reducing friction in case of fluid-film bearings.
- The use of low viscosity lubricants requires more control on the mating interfaces. Surface texturing, and controlling the surface roughness of both the bearings and the crankshaft, proved to be beneficial in terms of friction and wear reduction.
- Motored test rigs are being developed in order to simulate real operating conditions, to study the frictional behavior of isolated engine subsystems, such as main bearings.

Objectives

The main aim of the present work is the development and evaluation of a bench test method to test the frictional and wear performance of engine main bearings. The performance of the selected main bearings will be studied by generating friction data depending on:

- clearance
- load
- bearing top layer material
- surface roughness
- speed

Furthermore the friction and wear performance of the selected engine main bearings will be compared in order to rank the different bearing top layers. The bearing with the best performance will be also tested with a lower viscosity lubricant.

In the end all the varied test parameters will be analyzed in order to select the optimal combination.

Chapter 2

Materials and Experiments

This chapter aims to present in detail the different materials and specimens used in the experimental work.

First, the different specimen then the testing parameters will be presented, followed by the description of the testing procedure.

In the end, the method used for specimen characterization and the performed pre- and post-test analysis will be described.

2.1 Specimens and materials

Shaft

Two types of shafts, with different surface finish have been selected for the tests. One type of shaft specimen used was precipitation hardened steel, with a minimum hardness of 50 HRC according to specification and a surface finish of $R_a = 120$ nm. The second type, having a surface finish of $R_a = 60$ nm, was induction hardened steel, with a hardness ranging from 50-55 HRC, according to specification.

Bearing specimens

A bimetal lower bearing named A22E, with a chemical composition described in Table 2.1 - without top layer - was selected as reference bearing material.

Table 2.1: Chemical composition of A22E lower main bearings

Material	Main Composition (mass%)			
	Al	Sn	Si	Cu
A22E (lining)	balance	12	3.0	1.0

The second lower bearing material referred to as A10H, with the same chemical composition, but different mass % of additives (Table 2.2) had a top layer composed of a Bi surface and a silver intermediate layer. All upper bearing specimens had the same composition, as the AH10 bearing alloy, described in Table 2.2.

The A10H alloy is known to have a higher tensile strength, and therefore is expected

to have higher fatigue resistance, than the A22E alloy. On the other hand, A10H alloy has higher hardness than A22E, which is expected to lower conformability. According to literature [33] both are expected to show excellent seizure resistance, which can be attributed to the improved dispersion of Sn in the alloy.

The third bearing material (Table 2.3) was plated with two different polymer based top layers. One specimen had a top layer composed of PAI + MoS₂, while the second was composed of PAI+SiC+graphite.

Table 2.2: Chemical composition of A10H+PK1 lower main bearings.

Material	Main Composition (mass%)			
	Al	Sn	Si	Cu
A10H (lining)	balance	10	2.5	1.5
PK1 top layer	Ag intermediate layer	+	Bi	surface

Table 2.3: Chemical composition of polymer coated lower main bearings

Material	Main composition (mass%)				
	Al	Sn	Si	Cu	Cr
SA260 (lining)	balance	7	7	1.5	Zn
Polymer top layer 1					MoS ₂ + PAI
Polymer top layer 2					PAI+SiC+graphite

The bearings had a nominal outer diameter of 57 mm and inner radius of 53 mm. Their thickness is 2 mm, however it can vary slightly. The actual thickness of the main bearings is denoted by a color grade. The maximum thickness and minimum thickness for each color grade are shown in Table 2.4.

Table 2.4: Bearing thickness range for each color grade, in millimeters

	Minimum Thickness	Maximum Thickness
Red (R)	1.9900	1.9940
Yellow (Y)	1.9940	1.9980
Blue (B)	1.9980	2.0020
Green (G)	2.0020	2.0060

In conclusion, during the experimental work, four different types of main bearings materials have been tested for their friction and wear performance.

Lubricant

The two different lubricants used in the tests are the SAE 0W-20 and SAE 0W-16 oils. Both oils had the same additive package and only vary in viscosity. The temperature dependence of their density and viscosity are presented in Figure 2.1 - 2.3 and Figure 2.2 - 2.4. The presented data was given by the provider.

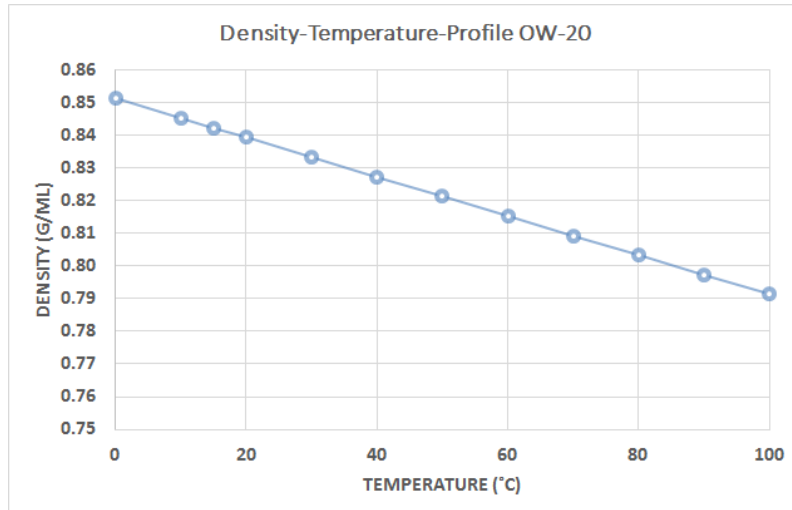


Figure 2.1: Variation of density as a function of temperature for the SAE 0W-20 engine oil.

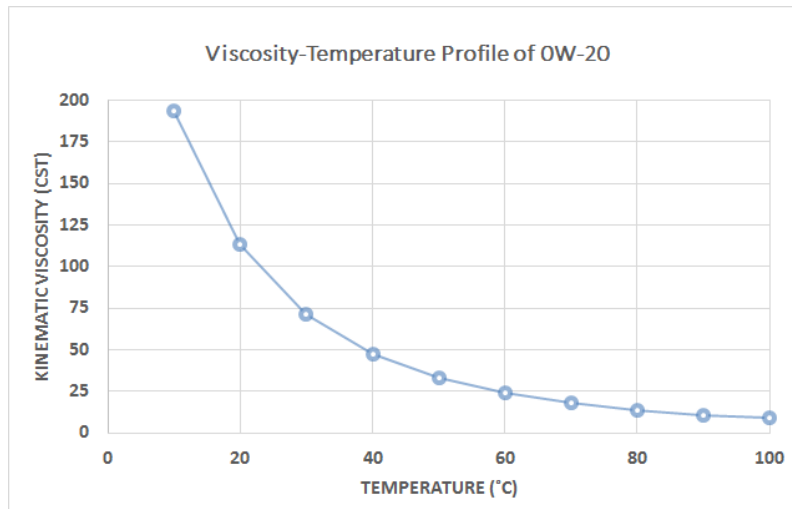


Figure 2.2: Variation of viscosity as a function of temperature for the SAE 0W-20 engine oil.

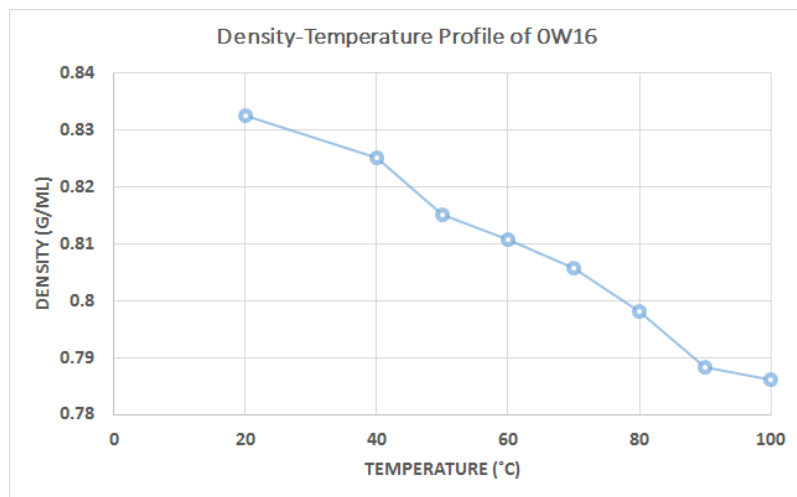


Figure 2.3: Variation of density as a function of temperature for the 0W-16 lubricant.

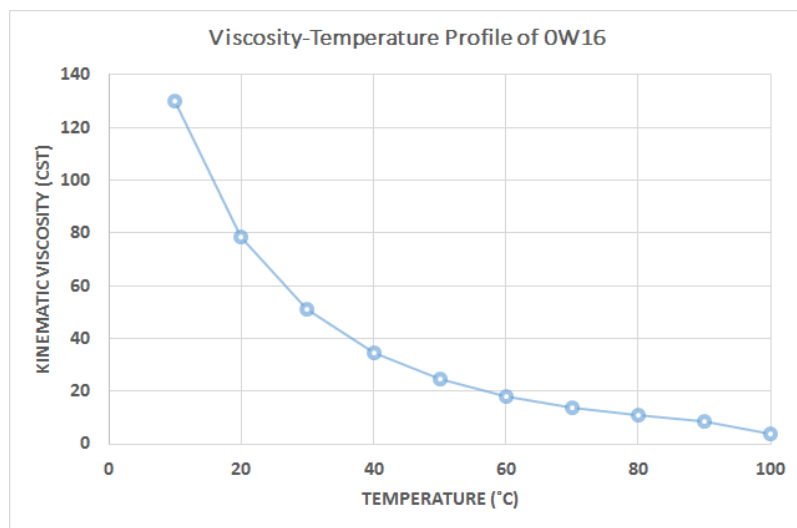


Figure 2.4: Variation of viscosity as a function of temperature for the 0W-16 lubricant.

2.2 Test parameters

The selected test conditions and parameters for the experimental study are listed in Table 2.5.

Table 2.5: Testing parameters for friction and wear tests.

Test Parameter	Test Type	Value
<i>Load</i>	<i>Wear test</i>	2000 N
	<i>Friction</i>	500 N & 2000 N
<i>Shaft speed</i>	<i>5x Stribeck curves</i>	(3000, 2700, 2300, 1700, 1200, 800, 500, 300, 200, 125, 75, 45, 20, 10) RPM
	<i>Wear test</i>	200
<i>Estimated contact pressure</i>	<i>Wear & Friction</i>	5 MPa (2000 N)
<i>Test duration</i>	<i>Friction</i>	30 min - pre-conditioning 45 min - testing
	<i>Wear</i>	90 min
<i>Test pattern</i>	<i>Friction</i>	pre-conditioning -, at 3000 RPM test - at 14 selected rotational speed
	<i>Wear</i>	test - rotation at constant speed 200 RPM
<i>Oil temperature</i>		80°C
<i>Shaft material</i>		Steel
<i>Shaft hardness</i>		min 50 HRC
<i>Shaft surface finish (Ra)</i>	<i>Friction & Wear</i>	120 nm & 60 nm
<i>Shaft diameter</i>		53 mm
<i>Bearing width</i>		19.4 mm
<i>Diametric clearance</i>		0.01 - 0.034 mm

2.3 Testing procedure

To test the performance of the selected bearing materials a modified twin disk test rig was used for generating friction data. The testing methodology was designed in such a way, that the resulting friction data can represent the bearing performance in different lubrication regimes.

The diametral clearance was varied by choosing the main bearings with different thickness from the four given color grades. The lower and upper part of the bearings was always selected from the same color grade.

Before each test, all specimens were cleaned with heptane followed by placing them in an ultrasonic bath for 10 minutes. Next, the lower and upper bearing specimens were mounted on the test rig and the selected load was applied. The performed friction and wear tests are summarized in Table 2.6. During these tests, the oil used to lubricate the system was the 0W-20 engine oil.

Table 2.6: List of conducted friction and wear tests.

Test series	Test type	Material	Shaft Ra [nm]	Bearing thickness	Load [N]
1.1.	<i>Friction</i> <i>5x Stribeck curves</i>	A22E	120	R, Y, B, G	500
1.2.			120		2000
2.1.			60		500
2.2.		A10H + PK1	120		2000
3.1			500		500
3.2			2000		2000
4.1		SA260 + Polymer 1	60		500
4.2			120		2000
5.1			60		500
5.2		SA260 + Polymer 2	60		20000
6.1	<i>Wear at 200 RPM</i>	A22E	120	R, Y, G, B	2000
6.2			60		
6.3		A10H+ PK1	120		
6.4			60		
6.5		SA260 + Polymer 2			

Each test was repeated three times, replacing the lower bearing specimens and keeping the same upper bearing specimen.

In the first tests, three bearing specimens were selected from each color grade. Diametral clearance was calculated, taking into account the variation in shaft diameter (Table 2.4).

Tests no. 1.1-1.2. were conducted in the same way, the only parameter that was changed was the applied load, which was increased from 500 N to 2000 N.

In test no. 2. the shaft was changed to the specimen with finer surface finish.

The tests were repeated choosing only one bearing thickness this time. The choice was made upon selecting the color grade giving a clearance value with the best friction performance.

In tests no. 3-5. only one bearing thickness was selected, using the same principle as described above. The bearing specimen having the A10H lining material coated with PK1 top layer, was tested with the shaft specimen having a rougher surface finish.

The two bearing materials with polymer coatings were tested with the smoother shaft specimen. The tests in series no. 6. were conducted in order to compare the wear performance and the break-away friction of the bearing materials.

In these tests, the rotational speed was kept constant at 200 rpm for 90 minutes, while the bearings were loaded with 2000 N during the test. The A22E bearing material without top layer was tested with all four bearing thicknesses, while the bearings coated with an overlay were tested selecting only one thickness. The shaft specimens had the same surface finish as in the friction tests.

After analyzing the data resulting from the tests listed in Table 2.6, the friction and wear tests were repeated using the lower viscosity lubricant, 0W-16.

2.4 Specimen characterization and analysis

The diameters of the shaft specimens were measured before the tests.

The clearance was determined in the following way. The upper and lower bearing specimens of the same color grade were placed in the bearing holder, and were clamped together with the specified force.

Next, a three-point internal micrometer was used to measure the inner diameters of the bearings fixed in the housing. The value of the clearance was calculated by subtracting the measured shaft diameter from the measured inner diameter of the bearing specimens.

Having the bearing thickness values given by their color grade, according to main engine bearing specification, the bearing specimens were selected to meet the desired clearance value.

The change in shaft surface roughness was documented, by analyzing the variation of the characteristic roughness parameters. Surface roughness measurements were performed with the Wyko 1100NT 3D optical profiler, using the vertical scanning interferometry method at a 10x magnification. The shaft surface was measured at two different position, at the center and also on the edge of the shaft. Surface roughness parameters, such as: **R_a**, **R_k**, **R_pk** and **R_vk** were documented before and after each test.

The surface of the tested bearings in the wear tests was analyzed with the help of surface topography characterization. Surface imaging was performed with the Zygo NewView 7300 3D profiler. Images were taken of both the original and the worn lower bearing surface.

Chapter 3

Results and Discussion

3.1 Design of the test rig

A test rig as shown in Figure 3.1 was developed and built to carry out the experiments.

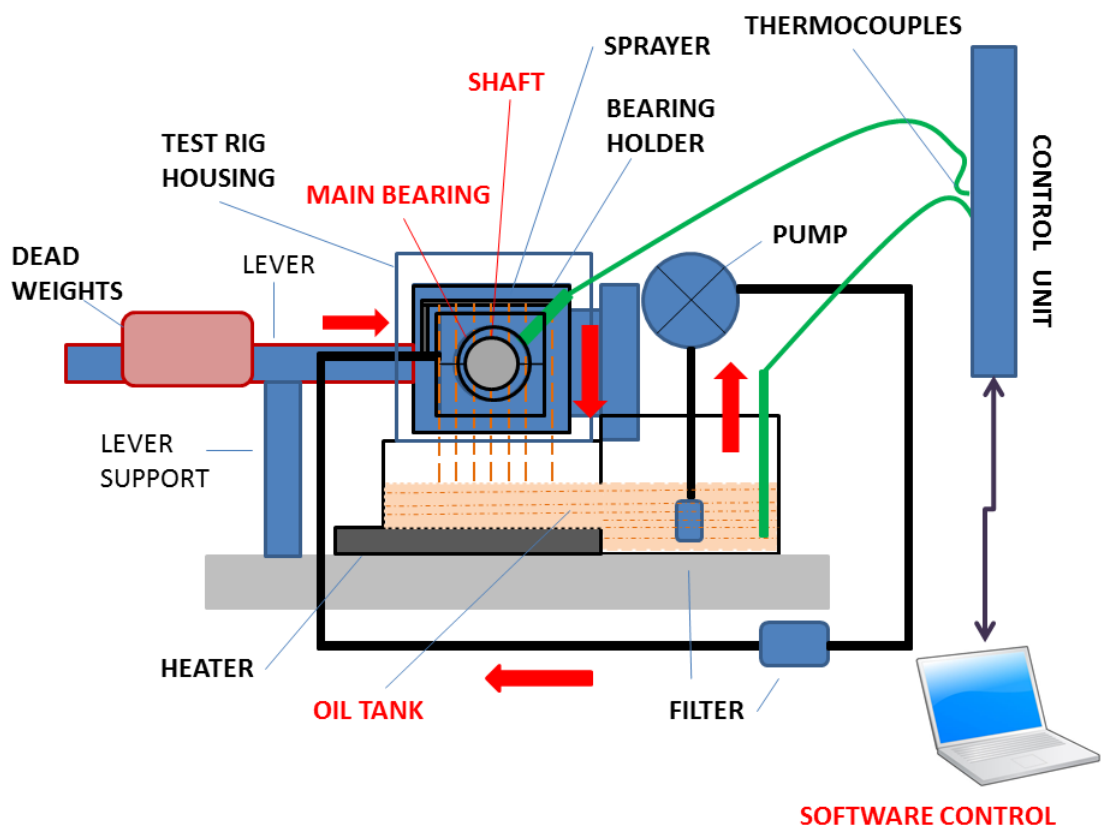


Figure 3.1: Conceptual set up of the test rig.

The test rig itself was a modified version of the WAZAU-UTM2000 twin-disk tribometer shown on Figure 3.2. The twin-disk tribometer has two different electric motor drives which are designed to rotate their respective shafts at different speeds from 0.1 to 3000 rpm. The modified version, developed for the experiments used one of the drives for rotating the shaft.

The interchangeable shaft specimen was positioned and fixed onto the drive's axle with a screw. Whereas the central shaft was driven by a motor fitted with a speed controller. The lower and upper bearings were assembled into the two separate parts of a designed bearing holder for the friction tests. The two separate parts could be clamped together with screws as shown in Figure 3.3 and Figure 3.4. The bearing holder was fixed to the second drive, the left arm of the twin-disk tribometer, and had a self aligning mechanism.

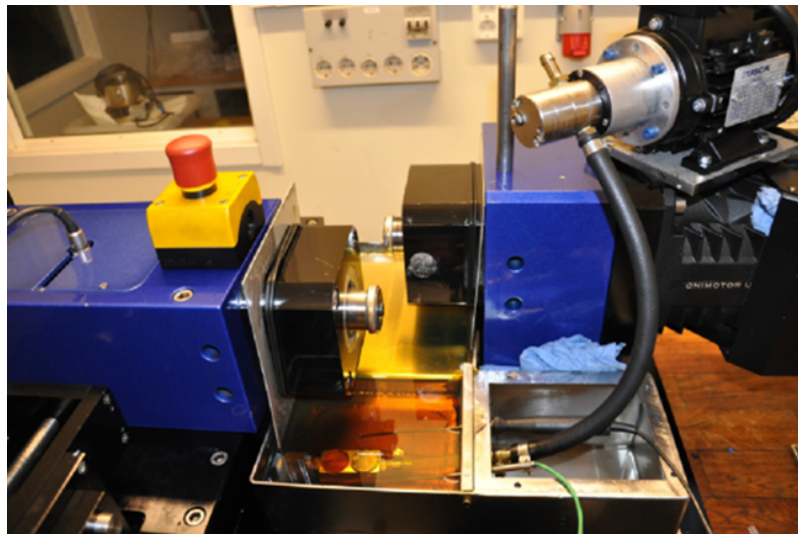
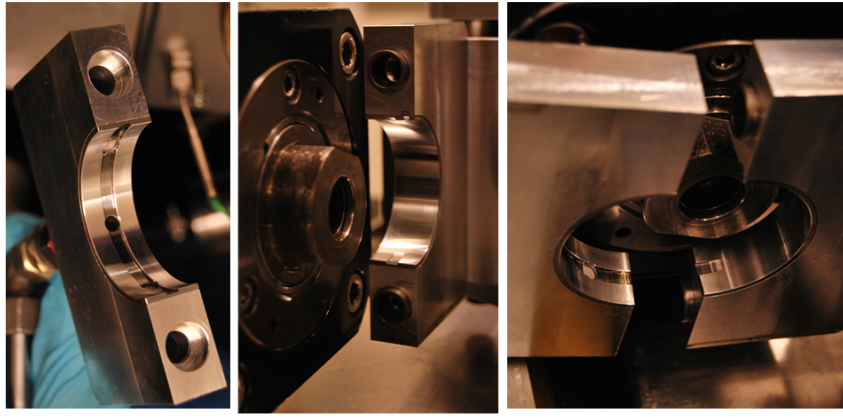


Figure 3.2: WAZAU-UTM2000 twin-disk tribometer.

An oil tank, equipped with a heater, was placed just below the bearing holder, collecting the lubricant squeezed out from the contact. The heater had temperature control realized by a thermocouple placed in the oil tank. A filter and a pump was connected to the oil tank, providing continuous and filtered lubricant supply to the holder on the side where the bearing shell with oil groove was fixed.

Additionally, a sprayer was attached to the bearing holder to spray hot oil on the housing to achieve more uniform temperature distribution around the tested specimen.

The bearing holder also had a hole drilled into it, where a K-type thermocouple was placed, touching the back of the lower main bearing, in order to measure the variation of temperature at the bearing back during friction and wear tests.



a).

b).

c).

Figure 3.3: Upper and lower main bearing specimen fixed in the bearing holders. a) The upper part - connected to the oil supply. b) The lower part. c) The disassembled bearing holder.

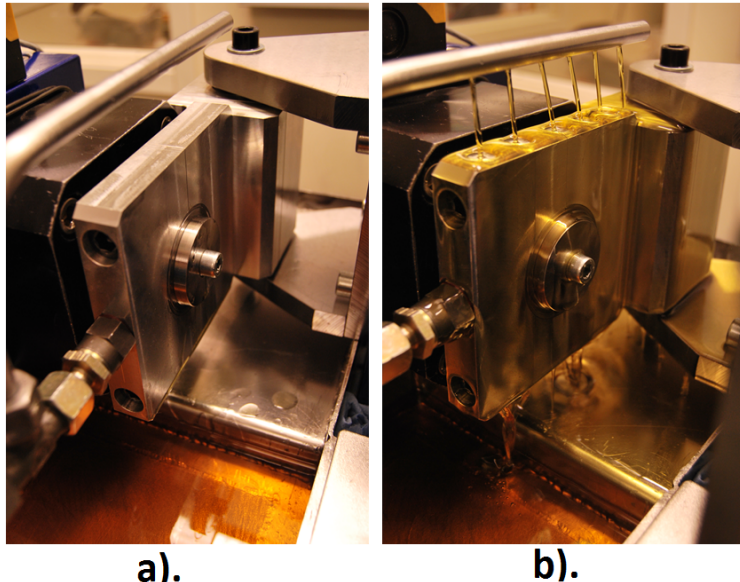


Figure 3.4: a) Assembled bearing holder around the shaft. b) Oil supply, and spraying mechanism.

The rig used dead weights to apply the load, and was equipped with and adjustable loading arrangement (Fig. 3.5). The load could be increased up to 2000 N. The tests were run through a program set up in a console interface from a computer. The data was collected with the help of a strain gauge torque sensor (Figure 3.6), containing a strain gauge to detect frictional torque acting on the shaft, which was then converted into the coefficient of friction and stored in the computer.

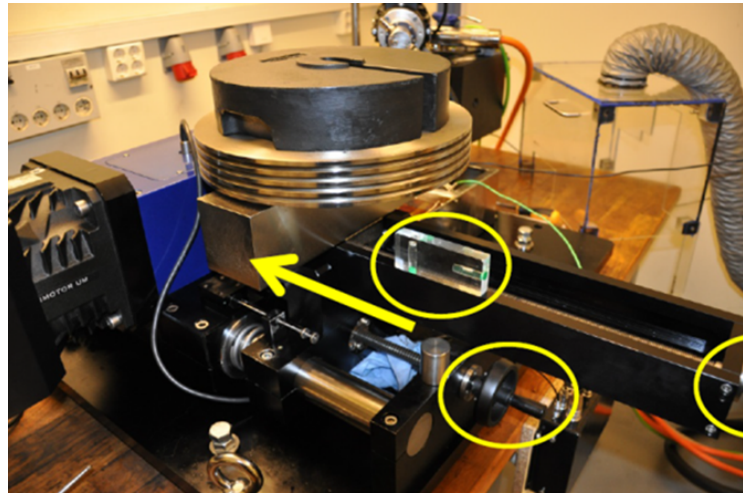


Figure 3.5: Loading arrangement

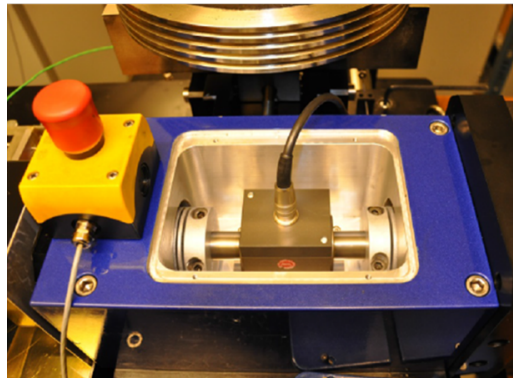


Figure 3.6: Friction torque sensor

3.1.1 Developed test methodology

The test parameters were chosen in such a way that the resulting friction data would cover all lubrication regimes.

The operating speed was decreased in steps, from 3000 rpm to 10 rpm. In total 14 different rotational speeds were chosen in order to provide representative curves .

At the beginning of each test, the shaft was left to rotate under testing load for half an hour at 3000 rpm with the aim of pre-conditioning. This way it could be ensured that the starting conditions are the same every time and the temperature is even around the bearing.

After half an hour, the rotational speed was decreased in the chosen steps until it reached 10 rpm.

From here speed was increased up to 3000 rpm, and decreased again in steps. At every chosen step, the speed was kept constant for 12 seconds and the friction torque data was averaged for 10 seconds. This sequence was repeated.

Consequently, series of Stribeck curves could be derived from the friction torque data. The friction coefficient was plotted as the function of the Hersey parameter, which was calculated using the measured bearing back temperature data to account for the variation in lubricant viscosity and density.

The number of repeats was chosen according to how fast the resulting Stribeck curves converged. In the figures included in the Appendix the five different curves, referred to as sweeps, resulting from the repeats are also presented.

The wear performance of the top layers was studied by running the tests in mixed-lubrication regime, at 200 rpm, for a longer period of time. This was followed by measuring the mass loss of the bearings after the tests.

3.2 Analysis of experimental data

In order to find the best performing bearing material, surface finish and lubricant combination among the selected samples for the experimental work, the analysis of the collected data is presented in the following order.

In the first part, the friction performances are shown as a function of applied load, bearing clearance, shaft surface roughness and bearings top layer material. In the second part, the results of the wear tests are presented as change of friction coefficient during test time and break away friction.

The friction and wear test results are followed by presenting the surface analysis. First, the change in shaft surface roughness parameters are shown. Last, the surface topography images of the original and tested bearings are presented.

At the end of the chapter, a summary of all test results is elaborated. The findings of the study are discussed in the summary.

3.2.1 Friction Performance

Al-Sn-Si-Cu (A22E) bearing alloy

In Figure 3.7 the Stribeck diagrams represent the bearing performance at 500 N and 2000 N loads. It can be seen that the results show the expected behavior in the different lubrication regimes.

The Stribeck diagrams with standard deviation values at each point are included in the Appendix (A3-A4). The points on the graph represent the averaged friction coefficients measured during the tests.

A small change in the Hersey parameter can be observed. This is due to the change in viscosity calculated by using the temperature variation in the contact, shown in the right corner of the graphs. The friction coefficient is relatively higher in both hydrodynamic and boundary regime under 500 N load.

Effect of load and clearance

The series of curves in Figure 3.8 represent the frictional behavior of the A22E bearing material for different clearances. The bearing specimen with the red color grade, gives the largest clearance around 0.035 mm, while the bearing with the green color grade gives the smallest clearance, around 0.01 mm.

It can be observed that the frictional behavior is relatively similar. Even though the diametral clearance is decreasing, the Stribeck curves follow the same trend. Evaluating the effect of load in the conducted tests, it was seen that by reducing the applied load to 500 N the coefficient of friction increased in the different lubrication regimes.

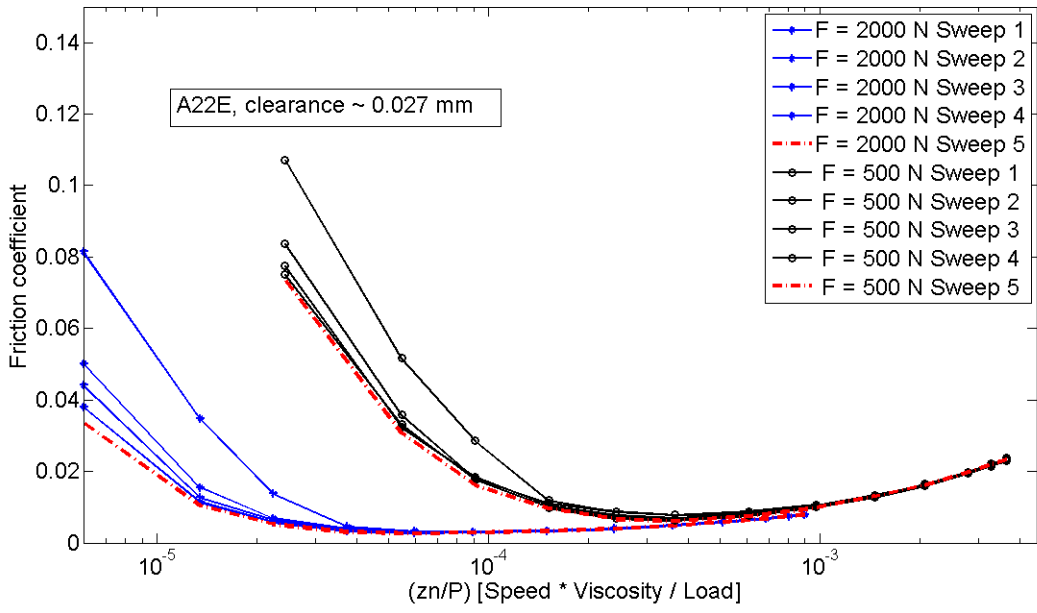


Figure 3.7: Test 1. Lubricant: 0W-20 engine oil, clearance: ≈ 0.027 mm. Stribeck diagram, representing the frictional performance of the A22E bearing material under 2000 N and at 500 N load (Appendices A3-A4).

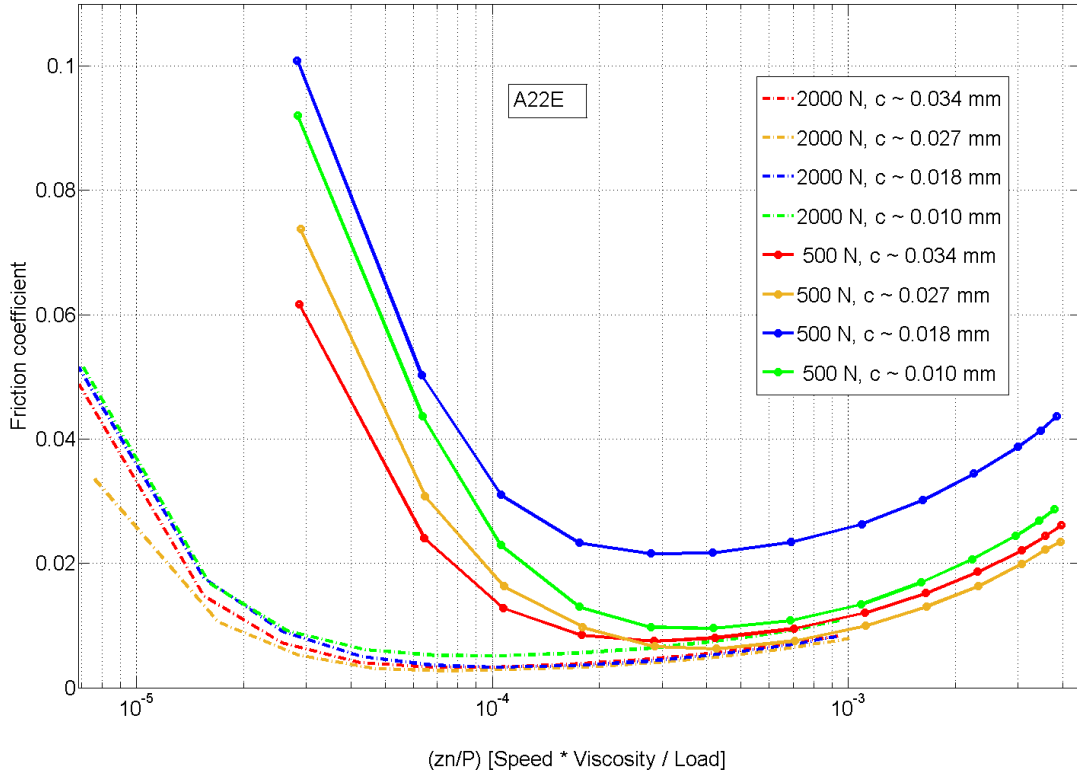


Figure 3.8: Test 1. Friction performance with 0W-20 engine oil. Stribeck diagrams, representing the frictional performance of the A22E bearing material under 2000 N and 500 N load respectively. The different curves represent the frictional behavior for different clearance values.

Effect of shaft surface roughness

Changing the shaft samples to shafts with finer surface finish resulted in higher friction in the boundary regime under 2000 N load, as can be seen from Figure 3.9.

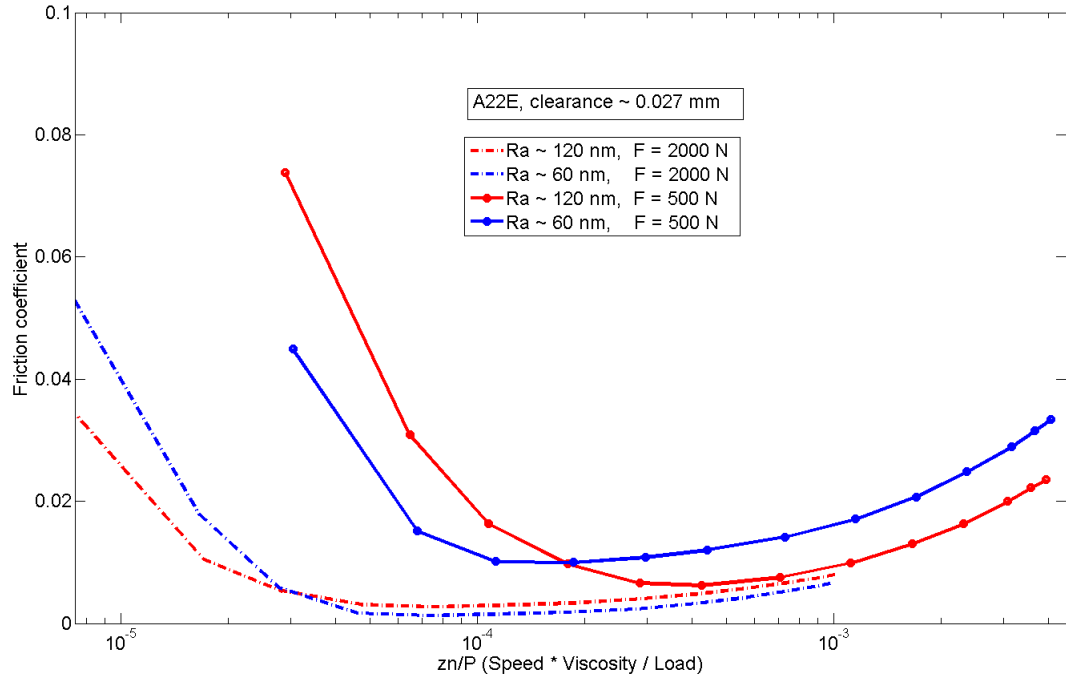


Figure 3.9: Tests 1.1.2, 1.2.2. and Test 2. Effect of shaft surface roughness. Lubricant: OW-20 engine oil, clearance: ≈ 0.027 mm. Results for two different shaft surface roughness $R_a \approx 120$ nm and $R_a \approx 60$ nm. Stribeck diagrams, representing the frictional performance of the A22E bearing material under different loads, 500 N and 2000 N respectively.

By comparing the last curve from each test, it can be seen, that at low load the difference in the frictional behavior, due to shaft surface roughness, is more pronounced than at high load. On the other hand, at higher loads the curves are overlapping each other, and the only considerable difference can be observed in the boundary lubrication regime.

3.2.2 Performance of bearing top layers

Al-Sn-Si-Cu (A10H) bearing alloy with PK1 top layer

The frictional performance of the PK1 top layer coated on the A10H bearing material under 500 N and 2000 N load, is presented below in Figure 3.10.

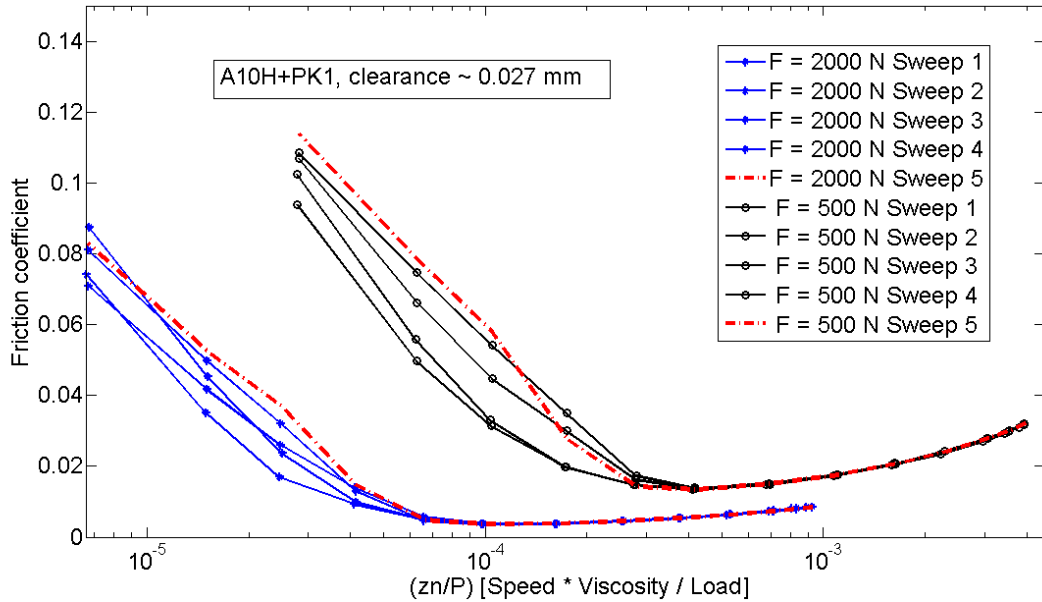


Figure 3.10: Test 3. Lubricant: 0W-20 engine oil, clearance: ≈ 0.027 mm. Stribeck diagram, representing the frictional performance of the A10H+PK1 bearing material under 2000 N and 500 N load(Appendices A9-A10).

Polymer based top layer - MoS₂ + PAI

The polymer top layers are coated on the third type of Al-Sn-Si-Cu bearing alloy, previously referred to as SA260. The effect of the polymer 1 top layer, having MoS₂ added to the PAI base, can be seen in Figure 3.11. At 2000 N load the newly

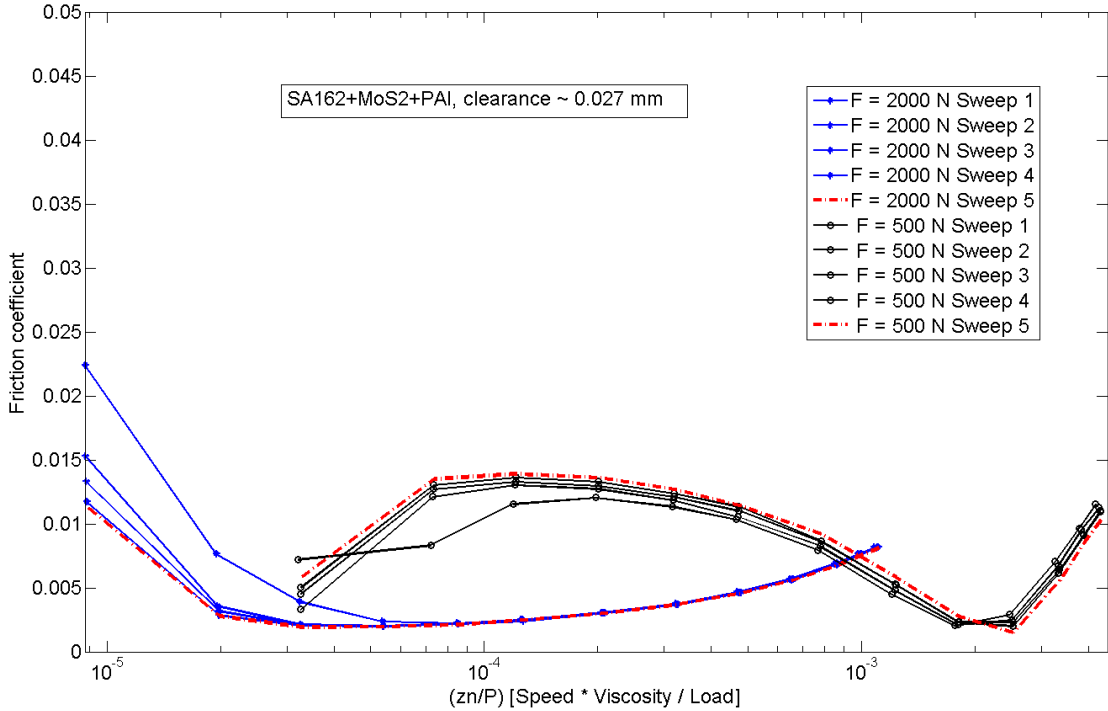


Figure 3.11: Test 4. Lubricant: 0W-20 engine oil, clearance: ≈ 0.027 mm. Stribeck diagram, representing the frictional performance of the SA260 bearing material coated with polymer based top layer MoS₂+PAI, under 2000 N and 500 N load (Appendices A11-A12).

developed PAI based top layer provides a noteworthy reduction in friction in the boundary regime. The friction coefficient measured at 500 N falls in the same range as the friction coefficient measured at 2000 N. However, the obtained results at 500 N show inconsistency compared to previous measurements at 500 N. The resulting Stribeck curves present unexpected behavior, which can be a result of improper test set up.

Polymer based top layer - PAI + SiC + graphite

Replacing MoS₂ and adding SiC with graphite to the PAI base in the top layer, results in relatively similar frictional performance under 2000 N load, when the two polymer coatings are compared.

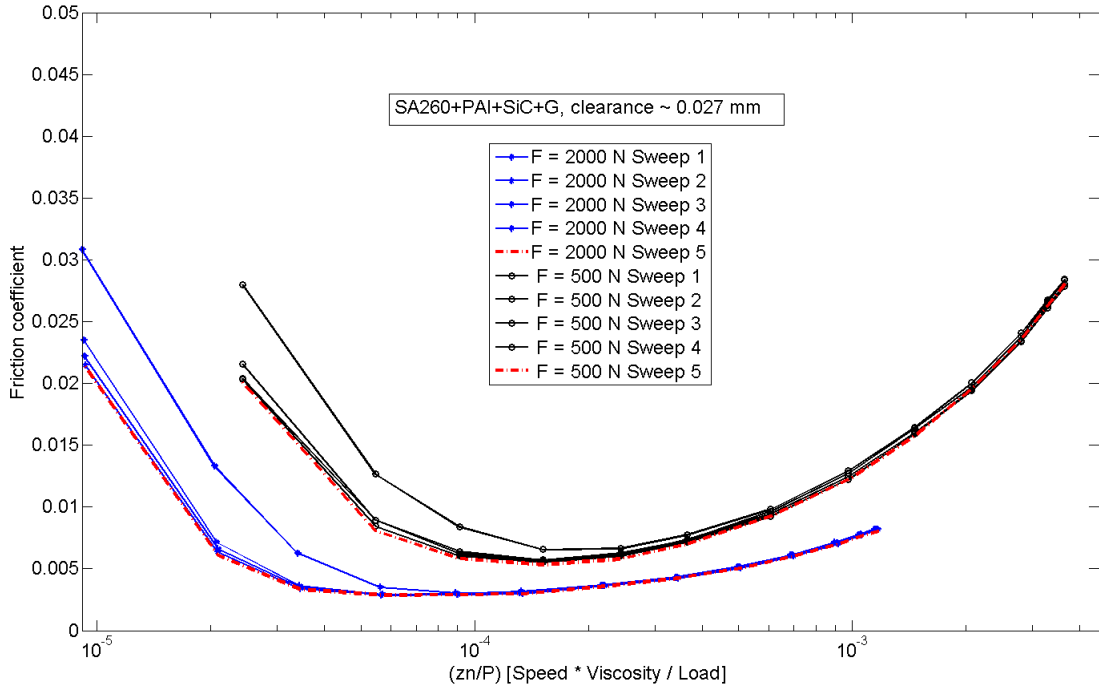


Figure 3.12: Test 5. Lubricant: 0W-20 engine oil, clearance: ≈ 0.027 mm. Stribeck diagram, representing the frictional performance of the SA260 bearing material coated with polymer based top layer PAI + SiC + graphite, under 2000 N and at 500 N load (Appendices A13-A14).

The polymer coating containing SiC and graphite (polymer 2), shows relatively higher friction coefficient at 500 N load, both in the boundary and hydrodynamic regime, as it can be seen in Figure 3.12.

On the other hand, the shape of the Stribeck diagrams resulting from the tests with the newly developed polymer coated bearings are slightly different compared to the curves from the tests with the A22E and A10H + PK1 bearing materials. The difference between the values of the friction coefficient in boundary and hydrodynamic regime is relatively small, compared to the tested non-polymer bearing materials.

3.2.3 Effect of lubricant viscosity - polymer top layer MoS₂ + PAI

The effect of lower viscosity lubricant on frictional performance is presented in Figure 3.13. The bearing material used in the tests with the low viscosity lubricant is the SA260 coated with the MoS₂+PAI polymer based top layer.

From the Stribeck diagram it can be seen that, at 2000N no change in friction coefficient between the viscosity grades 0W-20 and 0W-16 can be detected. Only in the boundary regime, the use of the lower viscosity lubricant seems to lead to an increase in friction. At 500 N the two curves representing the performance of the 0W-16 and 0W-20 oil do not follow the same trend and present inconsistent results. The discrepancy is caused by a measurement error which occurred during the friction tests conducted with 0W-20 engine oil.

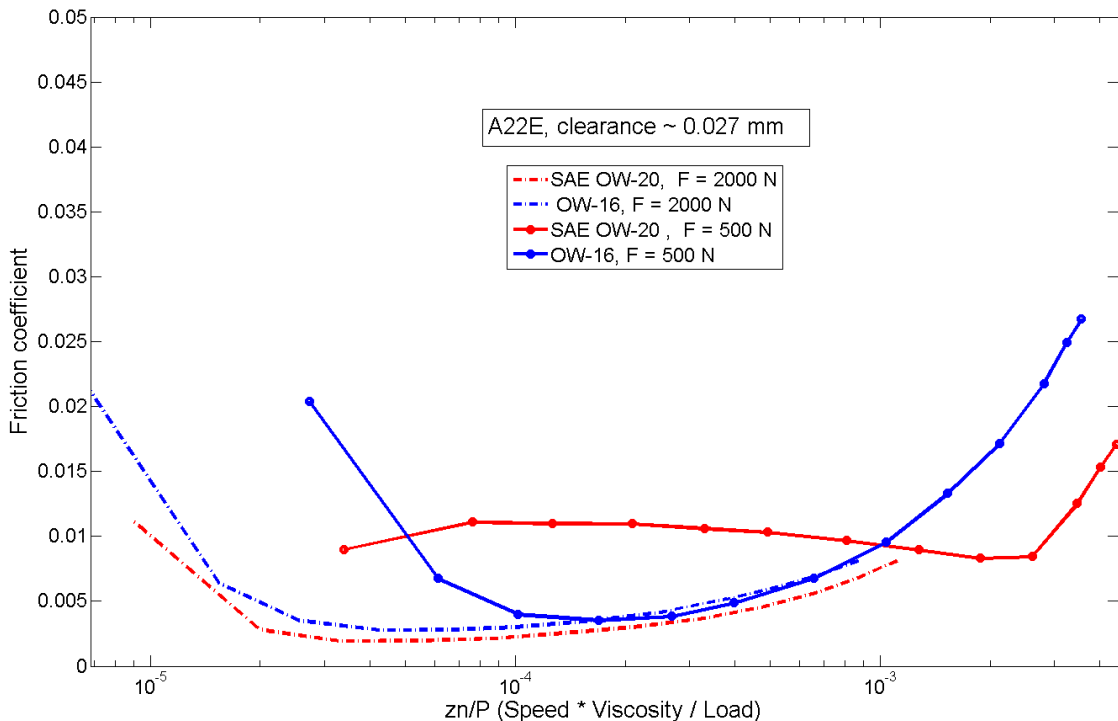


Figure 3.13: Lubricant: SAE 0W-16 oil, clearance: ≈ 0.027 mm. Stribeck diagram, representing the frictional performance of the SA260 bearing material coated with polymer based overlay MoS₂+PAI, under 2000 N and 500 N load respectively (Appendix A15-A16).

3.3 Running-in behavior and Wear performance

3.3.1 Effect of shaft surface roughness

The results from the wear tests representing the influence of shaft surface roughness, show that the surface finish can cause a notable decrease in the value of the break-away friction. As can be seen in Figure 3.14, the break-away friction drops from 0.17 to 0.05 when the shaft specimen with smoother surface is used.

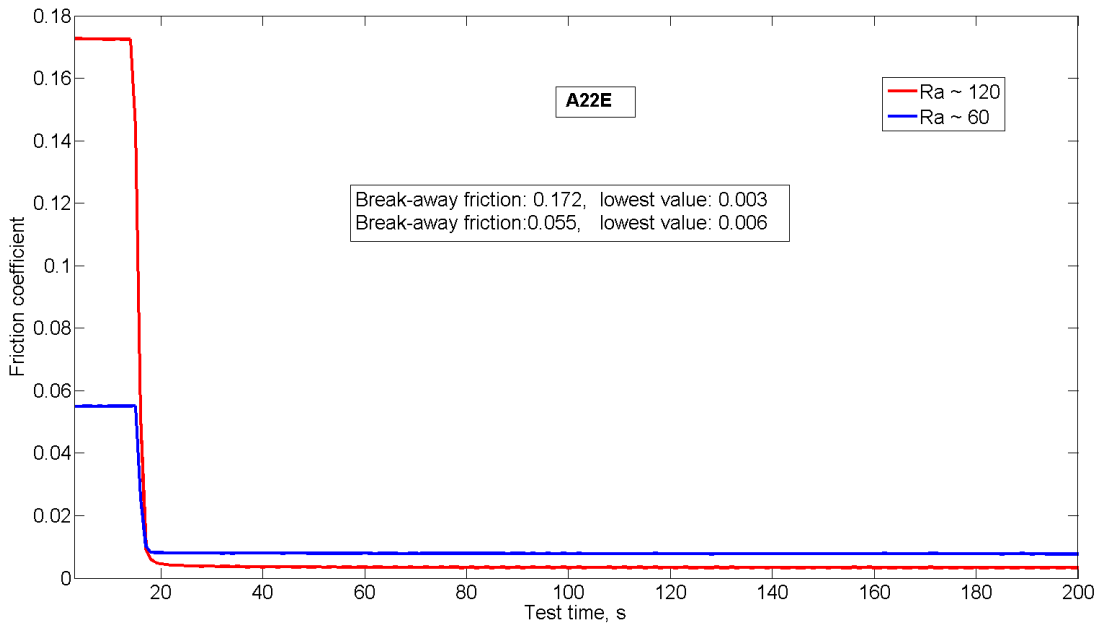


Figure 3.14: Tests 6.1. and 6.2. The running in behavior of the A22E bearing material, tested with the two shafts having different surface finish. Initial shaft surface roughness $Ra \approx 120$ and $Ra \approx 60$ respectively. Lubricant: 0W-20 engine oil, clearance: ≈ 0.027 mm.

3.3.2 Bearing top layer wear behavior

Looking at Figure 3.15, it can be seen that the break-away friction coefficient of A22E, is around 0.06 (tests with the shaft having a smoother surface finish). This value is lower than the break-away friction of the bearing with PK1 overlay, which is around 0.15.

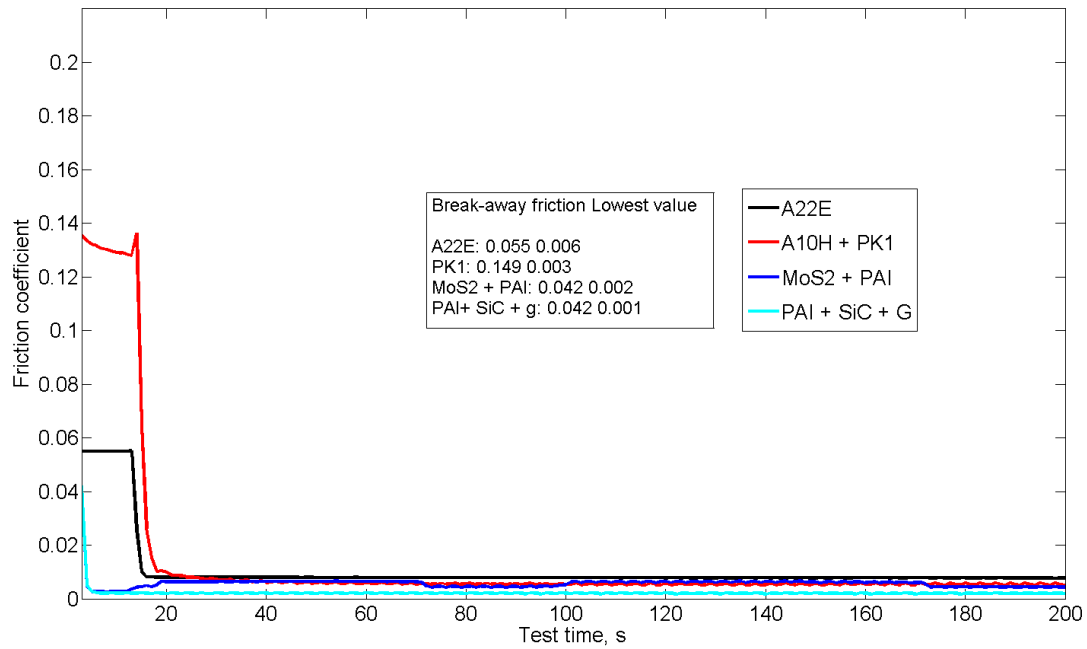


Figure 3.15: Test 6. Lubricant: 0W-20 engine oil, clearance: ≈ 0.027 mm. The running-in behavior of the different bearing materials.

After the wear tests the worn surface of the tested bearings showed visible changes. Compared to the reference bearing (Figure 3.16) the bearing with the PK1 top layer showed a worn out surface (Figure 3.17). The mass loss during these wear tests is summarized in the next section.

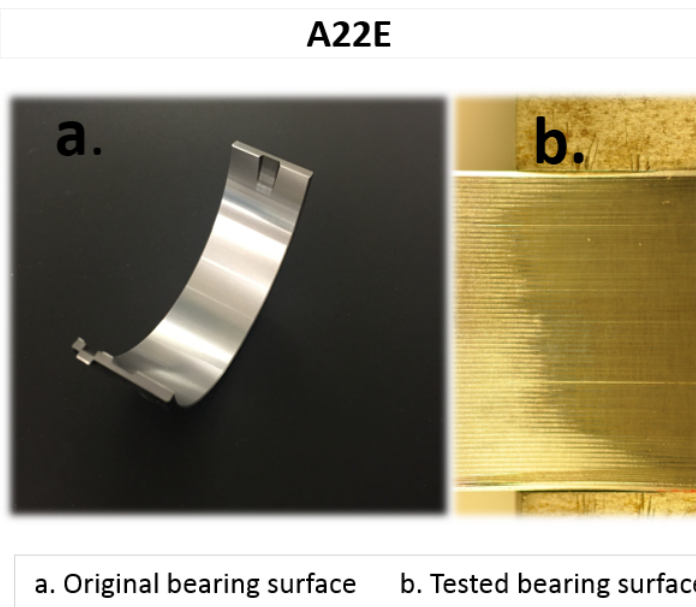


Figure 3.16: Test 6.1. Surface of the A22E bearing material after wear test. Lubricant: OW-20 engine oil, clearance: ≈ 0.027 mm.

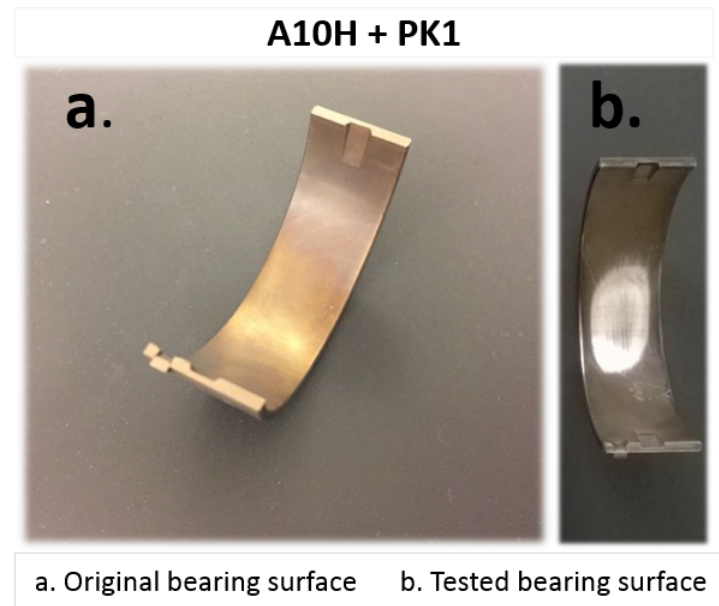


Figure 3.17: Test 6.3. Surface of the A10H + PK1 bearing material after wear test. Lubricant: 0W-20 engine oil, clearance: ≈ 0.027 mm.

The two polymer top layers showed similar behavior during the wear tests. Compared to the reference bearing material, the decrease in the break-away friction coefficient is relatively large, up to 20%, as can be seen from Figure 3.15.

On the surface of the polymer top layers no signs of severe wear could be observed during visual inspection. Moreover, the mass of the lower bearings coated with polymer based overlays showed relatively big variation after repeated measurements, therefore their wear behavior is not presented as mass loss.

3.4 Surface Analysis

Surface analysis results of the shaft and bearing specimen are presented in this section.

In case of the shaft specimens, the figures present the calculated average surface roughness parameters. The standard deviation indicates the change in surface roughness after each test. On the other hand, the surface of the bearing specimen can only be analyzed visually from the surface topography images.

3.4.1 Surface roughness measurements with 3D optical microscope

The changes in surface roughness of the shaft samples used in the different test series is presented on Figure 3.18 and Figure 3.19. The measured and averaged shaft surface roughness parameters (R_a , R_k , R_{pk} , R_{vk}) are shown in nanometers.

The surface roughness analysis indicates that, regardless of the bearing top layer, the changes on the surface occurred during the friction and wear tests are relatively small compared to the original surface roughness. Moreover, looking at the graphs which represent the change in the value of different roughness parameters, no trend or pattern can be recognized. Therefore, no direct correlation can be drawn between the change of shaft roughness and the friction data.

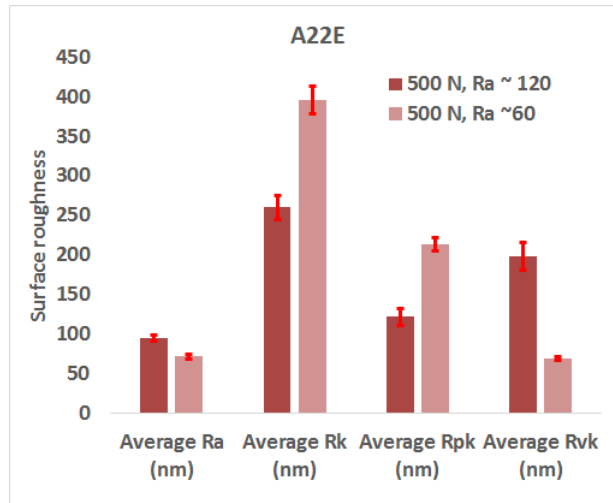


Figure 3.18: Test 1.1 2., and Test 2.1 Change of shaft surface roughness during friction test, under 500 N load. Comparing the two shafts with different surface finish. Represented by the average surface roughness and standard deviation. Bearing material: A22E; clearance: ≈ 0.027 mm; Lubricant: 0W-20 engine oil.

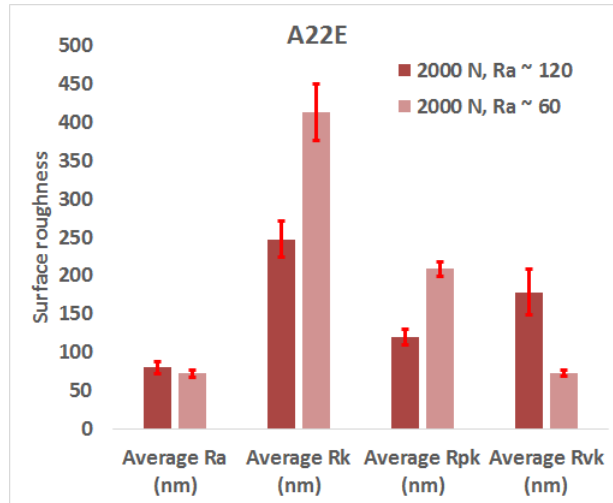


Figure 3.19: Test 1.2.2 and Test 2.2 Change of shaft surface roughness during friction test, full load, at 2000 N. Comparing the two shafts with different surface finish. Represented by the average surface roughness and standard deviation. Bearing material: A22E; clearance: ≈ 0.027 mm; Lubricant: 0W-20 engine oil.

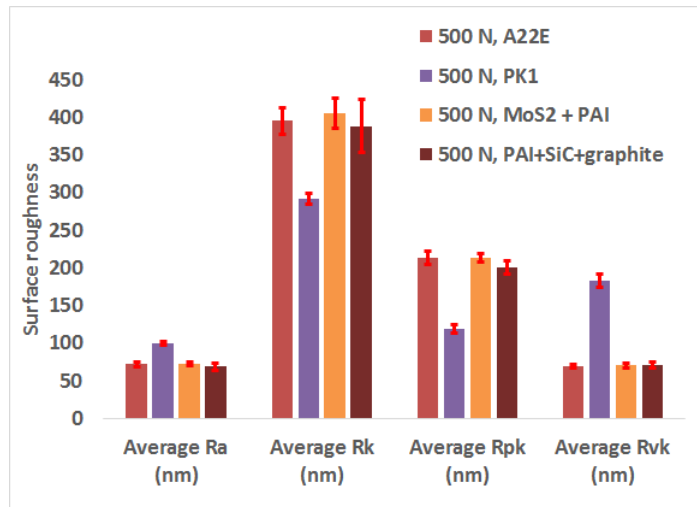


Figure 3.20: Tests 1-5. Change of shaft surface roughness during friction test, under 500 N. Comparing the effect of the different bearing materials. Represented by the average surface roughness and standard deviation. Clearance: ≈ 0.027 mm. Lubricant: 0W-20 engine oil.

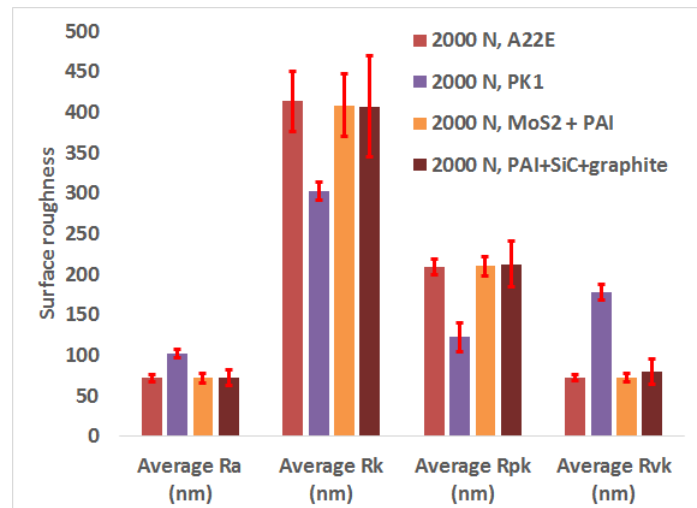


Figure 3.21: Tests 1-5. Change of shaft surface roughness during friction test, under 2000 N. Comparing the effect of the different bearing materials. Represented by the average surface roughness and standard deviation. Clearance: ≈ 0.027 mm. Lubricant: 0W-20 engine oil.

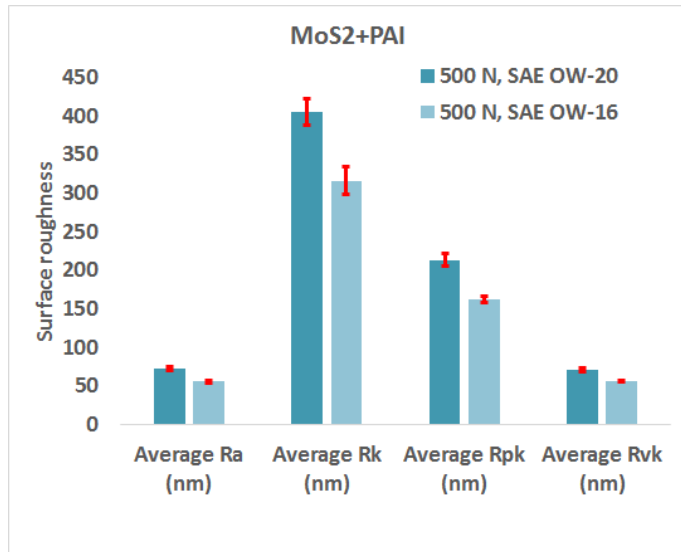


Figure 3.22: Effect of lubricant viscosity on the change of shaft surface roughness during friction test, under at 500 N. Represented by the average surface roughness and standard deviation. Bearing material: SA260+MoS₂+PAI, clearance: ≈ 0.027 mm.

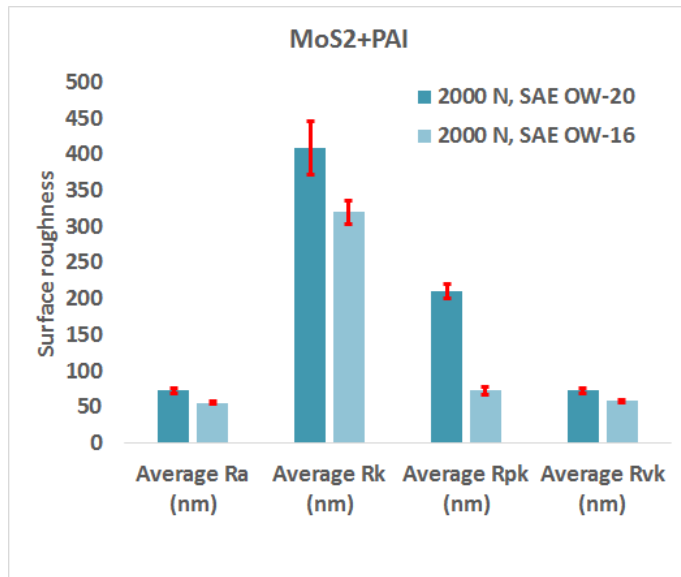


Figure 3.23: Effect of lubricant viscosity on the change of shaft surface roughness during friction test, under 2000 N. Represented by the average surface roughness and standard deviation. Bearing material: SA260+MoS₂+PAI, clearance: ≈ 0.027 mm.

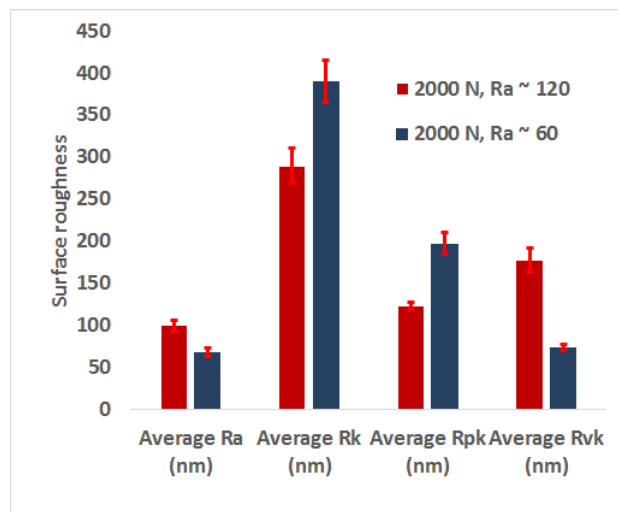


Figure 3.24: Test 6. Change in the shaft surface roughness during wear test. Represented by the average surface roughness and standard deviation. Comparing the two shafts with different surface finish. Clearance: ≈ 0.027 mm. Lubricant: 0W-20 engine oil.

3.4.2 Surface topography images

The surface topography images of the surface of the unused bearings compared to the surface of the tested bearings in the wear tests are presented below.

It can be seen that all bearings have a surface texture, in the form of microgrooves in the direction of sliding, which are meant to provide better lubrication.

The following images are aiming to represent how much the surface has changed during the wear testes compared to the original surface. In Figure 3.25 the surface of the reference bearing is presented. The lower bearing is one of the samples used in the wear tests lubricated with engine oil OW-20, and run with the shaft having a rougher surface.

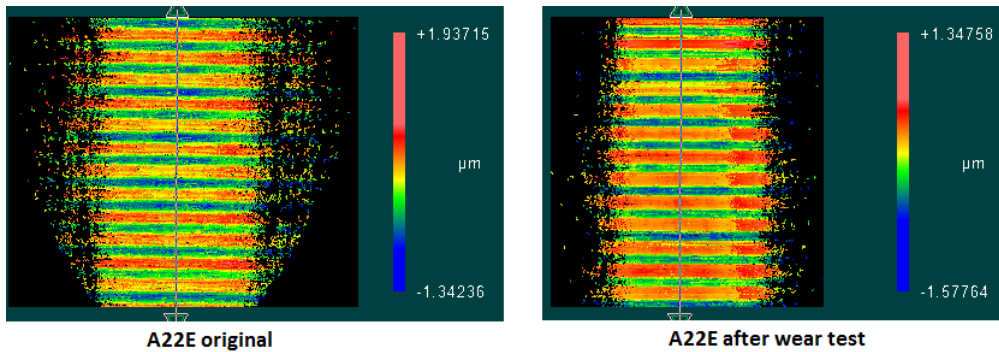


Figure 3.25: Test 6.1. Surface topography of the original A22E bearing surface compared to the tested sample. Tested with lubricant 0W-20. Original shaft roughness $R_a \approx 120$ nm.

Comparing the surface of the A10H+PK1 bearing after the wear tests to the reference bearing (Figure 3.26), it can be seen that there is a relatively bigger change in the topography, indicating a rougher surface after the tests.

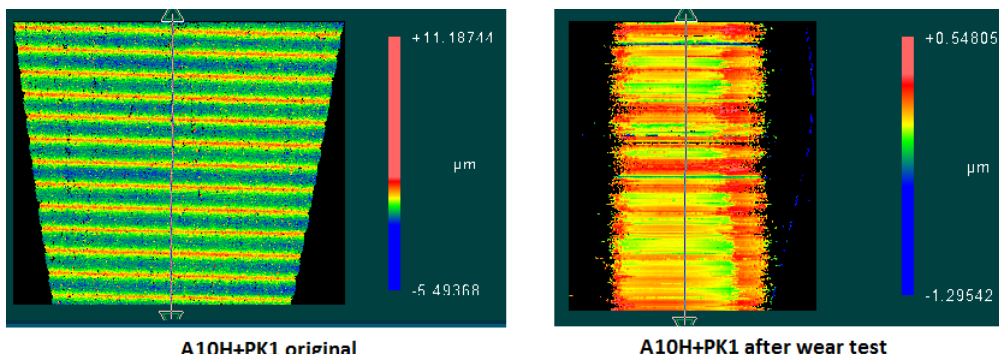


Figure 3.26: Test 6.3. Surface topography of the original A10H+PK1 bearing surface compared to the tested sample. Tested with lubricant 0W-20. Original shaft roughness $R_a \approx 120$ nm.

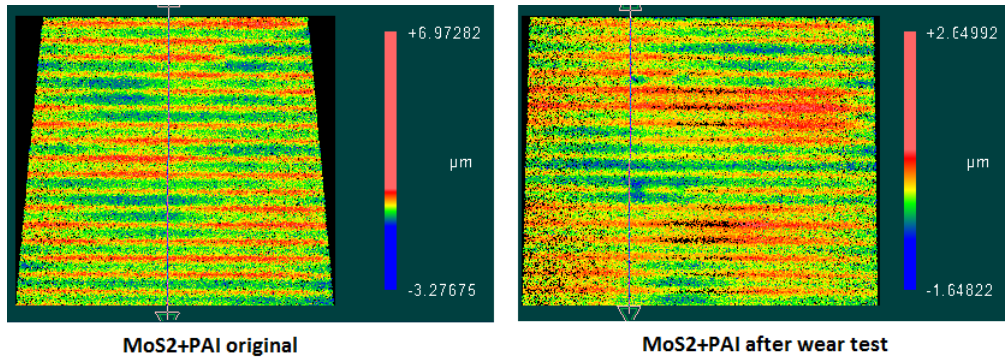


Figure 3.27: Test 6.4. Surface topography of the original SA260+MoS₂+PAI bearing surface compared to the tested sample. Tested with lubricant 0W-20.

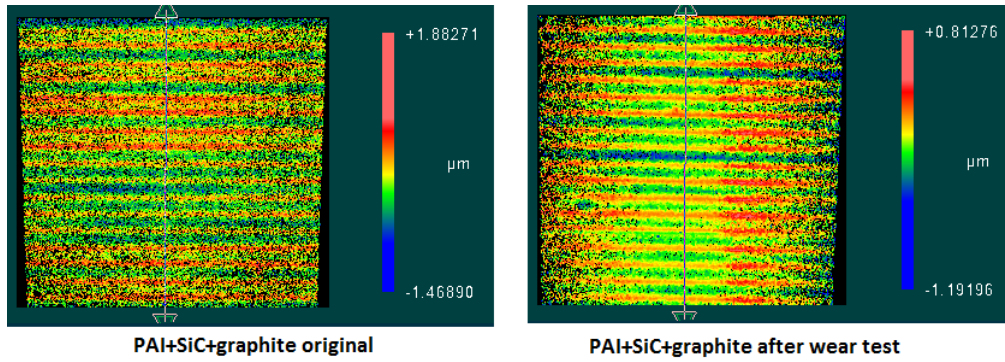


Figure 3.28: Test 6.5. Surface topography of the original SA260+PAI+SiC+graphite bearing surface compared to the tested sample. Tested with lubricant 0W-20. Original shaft roughness $R_a \approx 60$ nm.

The images taken of the bearing surfaces with polymer based top layers do not indicate severe change in roughness as it can be seen in Figure 3.28. However, looking at Fig. 3.29, the MoS₂+PAI polymer surface indicates a relatively higher roughness after the tests lubricated with 0W-16 lubricant.

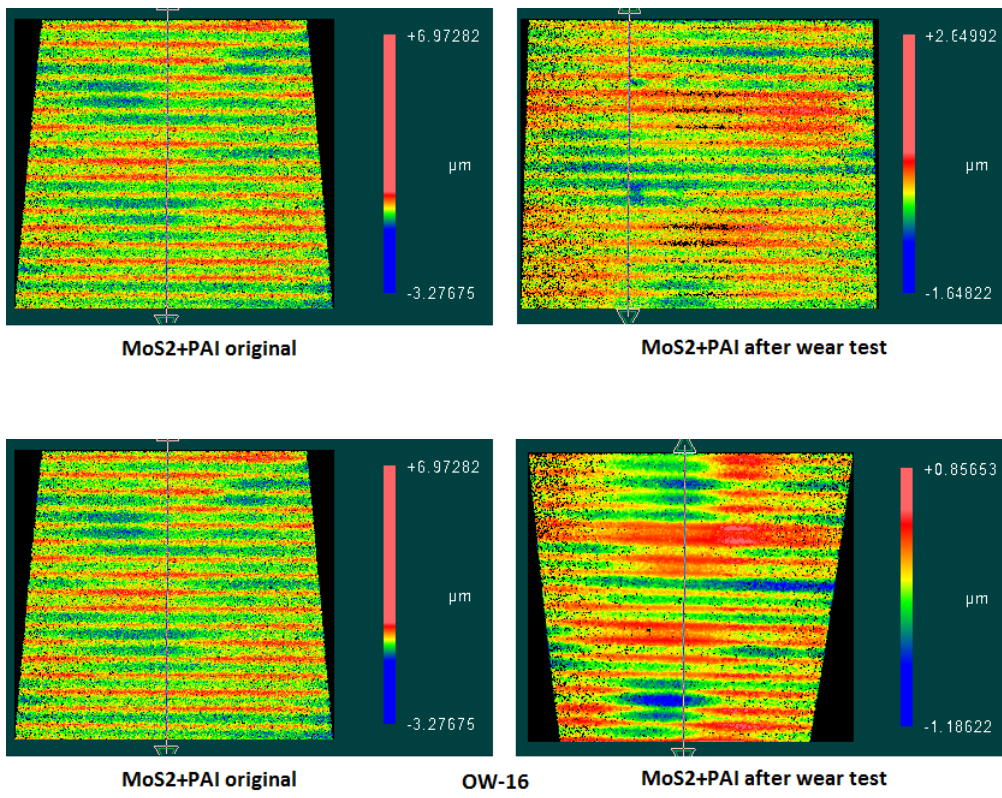


Figure 3.29: Surface topography of the original SA260+MoS₂+PAI bearing surface compared to the tested sample. Tested with lubricant OW-20 top images, and OW-16 bottom. Original shaft roughness $R_a \approx 60$ nm.

3.5 Summary and Discussion

In order to find the optimal parameters of the tested bearings, and to rank the different bearing top layers a comparative analysis has been proposed. The following summary aims to highlight the differences in frictional performance by including the influence of parameters such as applied load & rotational speed, diametral clearance, shaft surface roughness, bearing top layer and lubricant viscosity.

Friction performance

Reducing the load to 500 N in the friction tests, lead to an increase in the friction coefficient in the hydrodynamic regime. The effect can be related to the increase in film thickness under low loads. In case when there is a thicker film of lubricant separating the shaft and the bearing surface, the hydrodynamic friction is likely to increase due to the shearing of the lubricant film.

While the increase in frictional losses in the hydrodynamic region is expected, the Stribeck diagram shows a relatively higher friction coefficient in the boundary region as well.

The increase in the boundary region can be due to improper measurement set up (such as misalignment or temperature variation) which lead to inconsistent results. The seen behavior needs more detailed investigation in the future in order to find an explanation to it.

An alternative explanation for this behavior would be that the tested alloys and top layers are meant to provide good performance when they are exposed to higher loads. Reducing the applied load under a certain limit, could result in high friction since the functional surface, needs high loads and high temperatures in order to provide the expected performance. Furthermore, the interaction of the surface with the additives in the lubricant is also expected to happen at high loads and elevated temperatures.

Effect of clearance

From the theory of hydrodynamic lubrication it is expected that the frictional performance of the bearing to vary as a function of diametral clearance, both under high and low loads. In order to give a clear picture about the changes in frictional performance due to the effect of clearance, Table 3.1 and Table 3.2 lists the values of the average friction coefficient in different lubrication regimes.

These tables contain the starting and also the end value of the friction coefficient. BL_1 stands for the average value of the friction coefficient measured during the first sweep in boundary regime, while BL_5 stands for the value measured during the 5th sweep. Similarly HL_1 and HL_5 represent the values in the hydrodynamic regime.

From analysis of results presented in Table 3.1 and Table 3.2, it can be concluded that the diametral clearance with the value of $C \approx 0.027$ mm, provides the lowest friction, both under 500 N and 2000 N load.

Table 3.1: Values of the friction coefficient in different lubrication regimes as a function of diametral clearance, applied load 500 N.

A22E	500 N				
	min	BL ₁	BL ₅	HL ₁	HL ₅
C ~ 0.034 mm	0.007	0.107	0.061	0.025	0.026
C ~ 0.027 mm	0.006	0.107	0.073	0.023	0.023
C ~ 0.018 mm	0.009	0.134	0.092	0.028	0.028
C ~ 0.01 mm	0.021	0.144	0.1	0.042	0.043

Table 3.2: Values of the friction coefficient in different lubrication regimes as a function of diametral clearance, applied load 2000 N.

A22E	2000 N				
	min	BL ₁	BL ₅	HL ₁	HL ₅
C ~ 0.034 mm	0.003	0.081	0.048	0.008	0.008
C ~ 0.027 mm	0.002	0.081	0.033	0.007	0.007
C ~ 0.018 mm	0.003	0.108	0.051	0.008	0.008
C ~ 0.01 mm	0.005	0.103	0.051	0.01	0.01

Effect of shaft surface roughness

In the second test series, the influence of shaft surface roughness was investigated. The analysis was made by comparing the Stribeck diagrams (represented only by the 5th sweep) from the friction tests conducted with the two shaft samples, one having a surface roughness of $R_a \approx 120$ and the other $R_a \approx 60$.

Reducing the surface roughness affects the frictional performance differently under 500 N load, compared to operation under 2000 N load.

When the shaft was loaded with 500 N, the resulting values of the coefficient of friction are relatively higher in the hydrodynamic regime and smaller in the boundary regime. On the other hand, under 2000 N, the coefficient of friction is relatively higher in the boundary lubrication regime and smaller in the hydrodynamic regime.

Performance of the studied bearing top layers

The values of the friction coefficient in the different lubrication regimes are listed in Table 3.3 and Table 3.4. Starting with the representative values of the reference bearing, the tables also summarize the values of the coefficient of friction in case of the different bearing samples, coated with the bismuth- and the two polymer based top layers.

Table 3.3: Values of the friction coefficient in different lubrication regimes, compared to the A22E reference bearing material. Applied load 500 N. Lubricant 0W-20 engine oil.

C ~ 0.027 mm						
500 N	Ra (nm)	min	BL₁	BL₅	HL₁	HL₅
A22E	120	0.006	0.107	0.073	0.023	0.023
A22E	60	0.01	0.089	0.044	0.034	0.033
A10H+PK1	120	0.013	0.10	0.11	0.03	0.032
Polymer 1	60	0.001	0.007	0.005	0.011	0.01
Polymer 2	60	0.005	0.028	0.02	0.028	0.028

Table 3.4: Values of the friction coefficient in different lubrication regimes, compared to the A22E reference bearing material. Applied load 2000 N.

C ~ 0.027 mm						
2000 N	Ra (nm)	min	BL₁	BL₅	HL₁	HL₅
A22E	120	0.002	0.081	0.033	0.007	0.007
A22E	60	0.001	0.079	0.052	0.006	0.006
A10H+PK1	120	0.003	0.087	0.082	0.008	0.008
Polymer 1	60	0.001	0.022	0.011	0.008	0.008
Polymer 2	60	0.002	0.03	0.021	0.008	0.008

Comparing the values listed in Table 3.3 and Table 3.4, it can be clearly seen that the polymer based coating with MoS₂ provides the lowest friction in all lubrication regimes. The frictional performance of the three selected coatings is also presented in Figure 3.30 in the form of Stribeck diagrams represented by the last sequence (sweep) of every test.

Furthermore, looking at the diagram and the values of the friction coefficient from Table 3.3 and Table 3.4 it can be concluded, that the bearing with the bismuth based top layer provides the highest friction in the boundary lubrication regime.

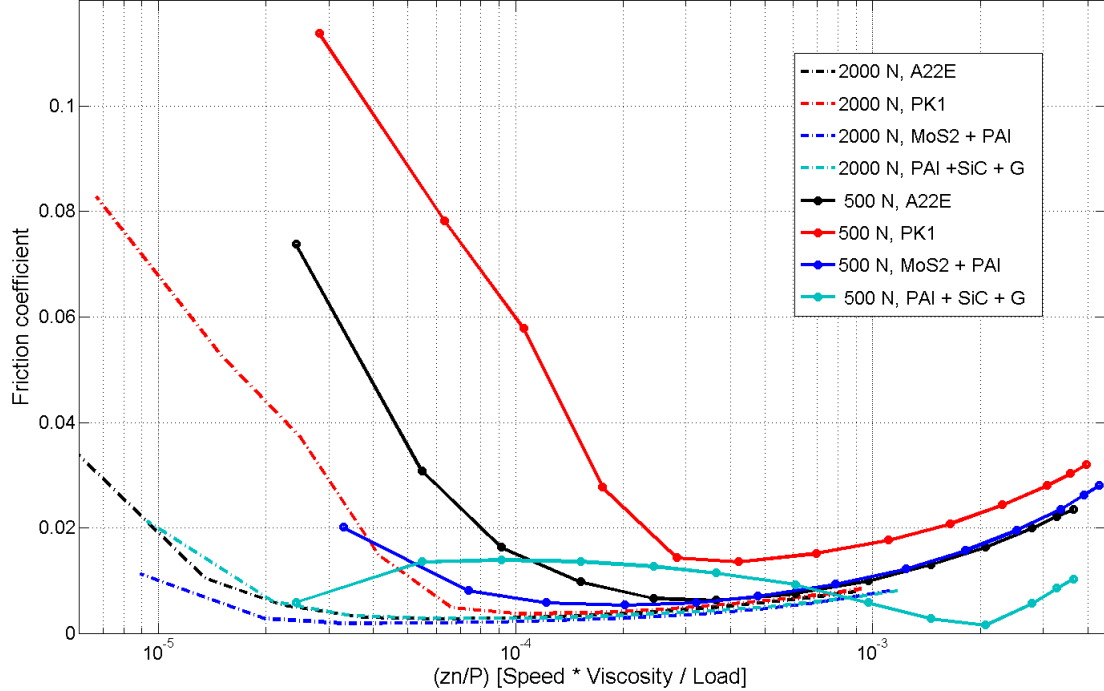


Figure 3.30: Frictional performance of the tested bearing materials and top layers. Tested with lubricant 0W-20. Original shaft roughness $R_a \approx 60$ nm.

When analyzing the performance of the two different polymer top layers, it can be seen that their frictional behavior is relatively similar when the applied load is 2000 N.

Effect of lower viscosity lubricant

Ranking the frictional performance of the top layer according to the data summarized in Table 3.3 and Table 3.4, the MoS₂+PAI polymer based coating was selected for the friction and wear tests lubricated with the lower viscosity lubricant.

The effect of lubricant viscosity, under running condition at 2000 N and 500 N load, is summarized in Tables 3.5 and 3.6.

Table 3.5: Values of the friction coefficient in different lubrication regimes. Sample: lower bearing coated with MoS₂+PAI. Comparison of frictional performance as a function of lubricant viscosity. Applied load 500 N.

<i>Polymer 1 : MoS₂+PAI</i>						
500 N	R_a (nm)	min	BL₁	BL₅	HL₁	HL₅
OW-20	60	0.001	0.007	0.005	0.011	0.01
OW-16	60	0.003	0.034	0.02	0.026	0.026

Table 3.6: Values of the friction coefficient in different lubrication regimes. Sample: lower bearing coated with MoS₂+PAI. Comparison of frictional performance as a function of lubricant viscosity. Applied load 2000 N.

<i>Polymer 1 : MoS₂+PAI</i>						
2000 N	R_a (nm)	min	BL₁	BL₅	HL₁	HL₅
OW-20	60	0.001	0.022	0.011	0.008	0.008
OW-16	60	0.002	0.036	0.021	0.008	0.008

By studying the values of the friction coefficient listed in Table 3.5 and Table 3.6, it can be seen that the lower viscosity lubricant does not provide a better frictional performance under 500 N load. When the load is increased to 2000 N, the two representative Stribeck curves overlap each other. The test results with the OW-16 lubricant show a slightly higher friction in the boundary regime.

Wear performance of the top layers

By comparing the wear performance of the selected top layers, the following can be summarized. The diametral clearance does not have a notable influence on the amount of wear, as it can be seen in Figure 3.31. Compared to the reference bearing material the amount of wear in case of the bismuth based top layer is considerably higher. As was seen in Figure 3.17 in the previous section, the top layer is worn out after the wear tests.

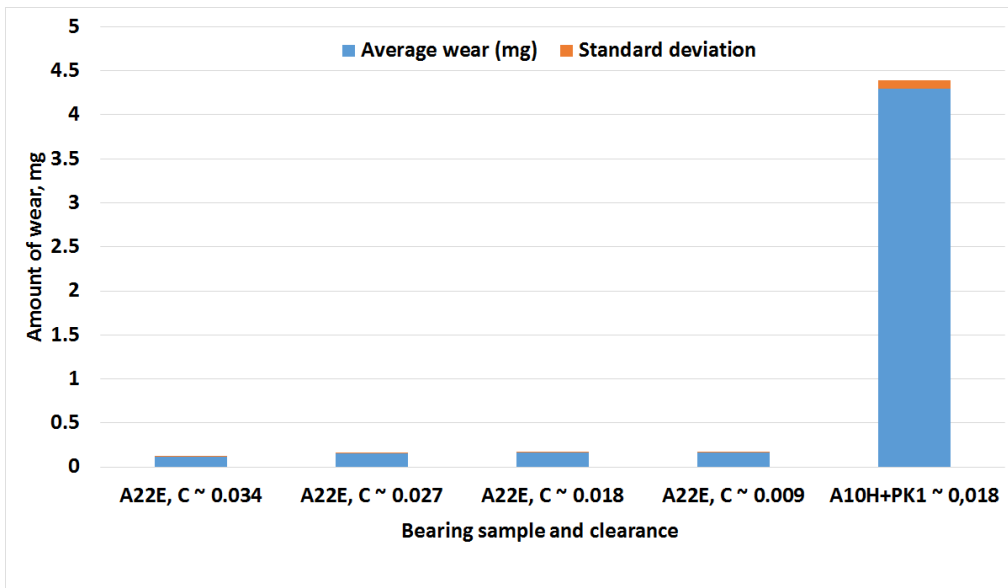


Figure 3.31: Wear as amount of mass loss in case of the A22E bearing material tested at different clearance values, and in case of A10H+PK1 bearing material tested at a clearance ≈ 0.018 mm. Original shaft roughness, $R_a \approx 120$ nm.

Using a shaft with a smoother surface finish shows beneficial effects in case of the wear performance. As can be seen on Figure 3.32 the amount of wear is relatively smaller after the wear test with the shaft samples having a R_a value around 60 nm.

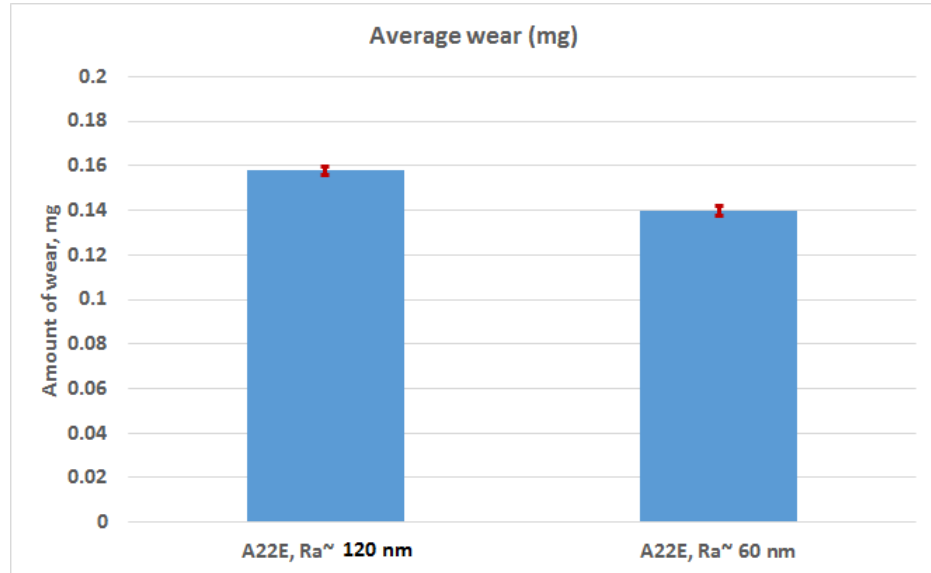


Figure 3.32: Wear performance represented by the amount of mass loss in case of the A22E lower bearing material, tested at a clearance $\approx 0.027 \text{ mm}$. Effect of shaft surface finish on the wear performance.

Chapter 4

Conclusions

The development of a test rig, by suitably modifying a twin disc machine for conducting tests on engine main bearings was carried out with success.

This test rig has been utilized to conduct extensive studies on different engine bearings under different operating conditions when lubricated with different engine oils. The salient conclusions of this study are as follows:

Comparing all the results representing the frictional behavior at 500N and 2000N it can be concluded that the measurement method is more consistent at 2000N. Under 500 N load multiple measurements showed discrepancies which need to be investigated in the future. The seen discrepancy in the case of the bearing with PAI + MoS₂ top layer is due to an error that occurred during the measurement.

The temperature measurements on bearing back bearing provides data only with a good approximation, therefore the variations in accuracy needs to be taken into account.

In conclusion, the test rig is able to generate reliable friction data at 2000 N under lubricated conditions depending on diametral clearance, shaft surface finish and lower main bearing top layer.

Taking into account the measurement only under 2000 N load, from the presented experimental work, the following conclusions can be drawn:

- The diametral clearance has an influence on the frictional losses. The test results show that among the selected clearance values, the clearance of around 0.027 mm provides the optimal performance.
- The surface finish of the shafts has only a relatively small influence on the frictional performance.
- The lower main bearing with the PK1 bismuth based top layer shows higher friction and wear among the tested bearings. However, the measured high friction coefficient drops significantly in short period of time at constant rotational speeds, showing an improved performance at a cost of high friction and wear during running-in.

- The polymer based top layers show remarkable performance, up to 20% reduction in friction in the boundary regime, compared to the reference bearing material.
- Lubricating the bearings with lower viscosity oil does not show notable improvement in reducing the frictional losses.
- The value of the clearance does not have a notable influence on the wear performance.
- The wear tests show that the smoother shaft surface finish provides a small reduction in material loss due to wear.
- The amount of wear is found to be 20-times higher in the case of the bismuth based top layer, compared to the reference bearing.
- The wear performance of the polymer top layers could not be evaluated in the form of mass loss. Surface topography images indicate that there is only a small change in surface roughness after the wear tests.
- At a clearance of around 0.027 mm the MoS₂ + PAI polymer based top layer, lubricated with 0W-20, provides the most notable reduction in friction losses in the boundary lubrication regime, while the PK1 -bismuth based top layer has a high running-in friction accompanied by increased wear.

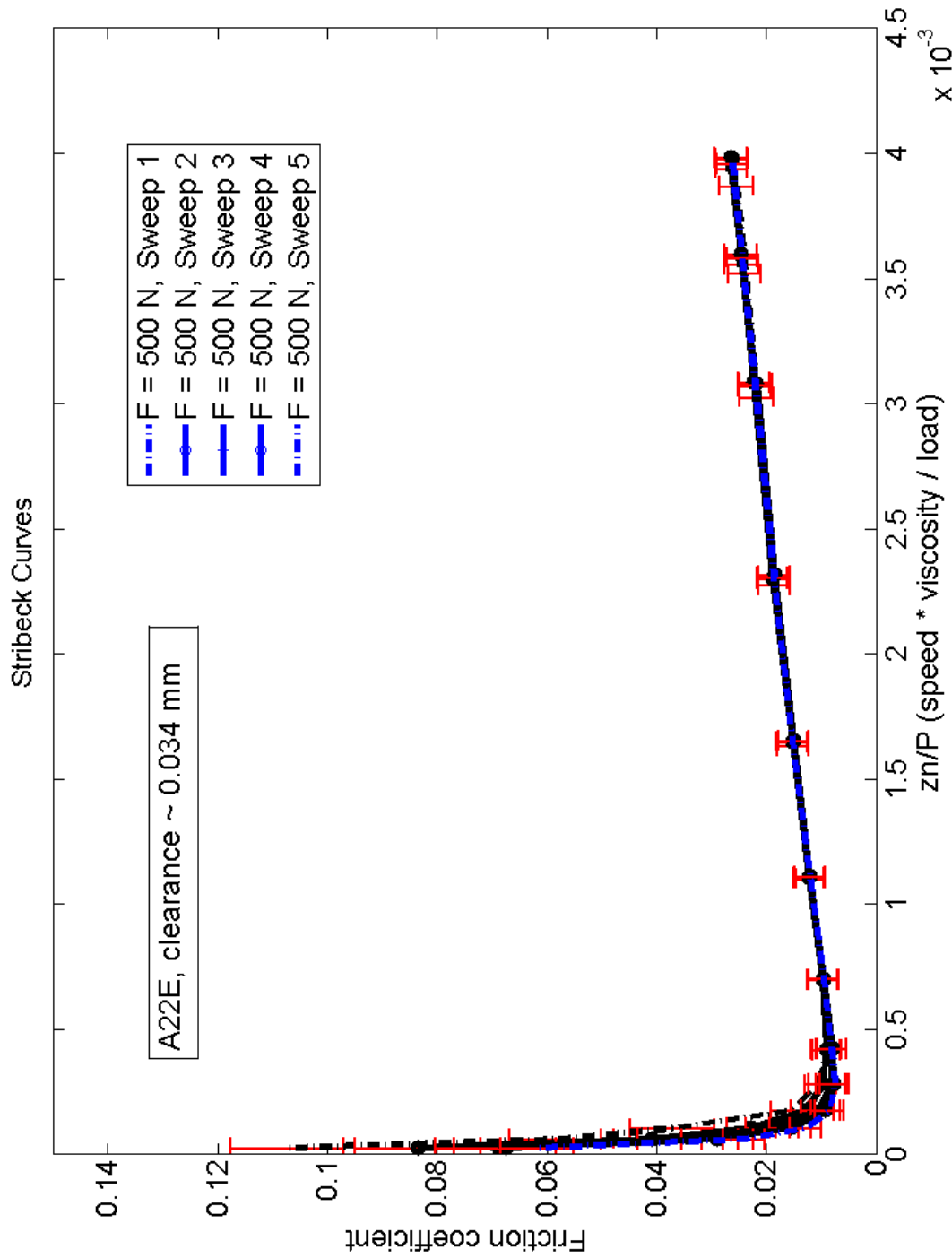
Bibliography

- [1] D. Duncan Dowson. *History of tribology*. Longman, 1979.
- [2] H Peter Jost and J Schofield. Energy saving through tribology: a techno-economic study. In *Institute of petroleum. Meeting*, pages 009–82, 1982.
- [3] Evaluation of regulations 443/2009 and 510/2011 on co2 emissions from light-duty vehicles. http://ec.europa.eu/clima/policies/transport/vehicles/docs/evaluation_ldv_co2_regs_en.pdf. Accessed: 2016-03-10.
- [4] Directive 2011/65/eu of the european parliament and council on the restriction of the use of certain hazardous substances in eee. <http://eur-lex.europa.eu/legal-content/EN/TXT/?uri=CELEX:32011L0065>. Accessed: 2016-03-10.
- [5] Yuji Enomoto and Takashi Yamamoto. New materials in automotive tribology. *Tribology Letters*, 5(1):13–24, 1998.
- [6] Kenneth Holmberg, Peter Andersson, and Ali Erdemir. Global energy consumption due to friction in passenger cars. *Tribology International*, 47:221–234, 2012.
- [7] PA Lakshminarayanan and Nagaraj S Nayak. *Critical component wear in heavy duty engines*. John Wiley & Sons, 2011.
- [8] Rasish Khatri and Dara W Childs. An experimental investigation of the dynamic performance of a vertical-application three-lobe bearing. *Journal of Engineering for Gas Turbines and Power*, 137(4):042504, 2015.
- [9] Understanding journal bearings. http://edge.rit.edu/edge/P14453/public/Research/2-_LEADER_-_Understanding_Journal_Bearings.pdf. Accessed: 2015-12-10.
- [10] Engine bearings and how do they work king engine bearings. http://kingbearings.com/files/Engine_Bearings_and_How_They_Work.pdf. Accessed: 2015-12-10.
- [11] Optimization of clearance design for high performance engine bearings. http://www.substech.com/dokuwiki/doku.php?id=optimization_of_clearance_design_for_high_performance_engine_bearings. Accessed: 2015-12-10.
- [12] Christopher Malcolm Taylor. *Engine tribology*, volume 26. Elsevier, 1993.

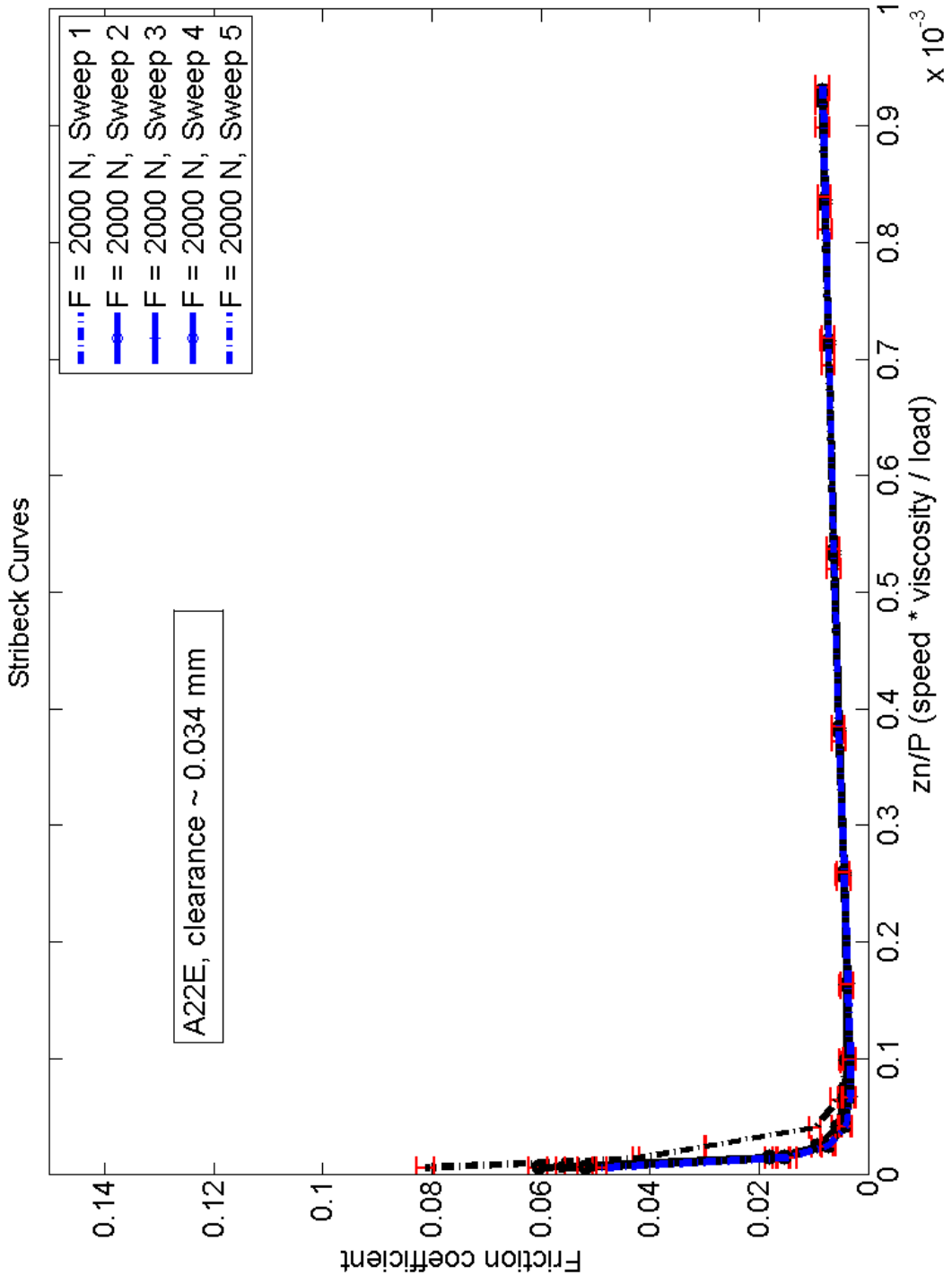
- [13] Bearings in internal combustion engines. http://www.substech.com/dokuwiki/doku.php?id=bearings_in_internal_combustion_engines. Accessed: 2015-12-10.
- [14] Dominique Bonneau, Aurelian Fatu, and Dominique Souchet. *Internal Combustion Engine Bearings Lubrication in Hydrodynamic Bearings*. John Wiley & Sons, 2014.
- [15] Mustapha Lahmar, Djamel Frihi, and Daniel Nicolas. The effect of misalignment on performance characteristics of engine main crankshaft bearings. *European Journal of Mechanics-A/Solids*, 21(4):703–714, 2002.
- [16] Jianbin Luo, Yonggang Meng, Tianmin Shao, and Qian Zhao. *Advanced tribology: proceedings of CIST2008 & ITS-IFTOMM2008*. Springer Science & Business Media, 2010.
- [17] Michael M Khonsari and E Richard Booser. *Applied tribology: bearing design and lubrication*, volume 12. John Wiley & Sons, 2008.
- [18] Qian Wang and Yip-wah Chung. *Encyclopedia of tribology*. Springer New York, 2013.
- [19] AE Bravo, HA Durán, VH Jacobo, A Ortiz, and R Schouwenaars. Towards new formulations for journal bearing alloys. *Wear*, 302(1):1528–1535, 2013.
- [20] T Rameshkumar and I Rajendran. Mechanical and tribological properties on al-sn-si alloy-based plain bearing material. *Tribology Transactions*, 56(2):268–274, 2013.
- [21] GC Yuan, ZJ Li, YX Lou, and XM Zhang. Study on crystallization and microstructure for new series of al-sn-si alloys. *Materials Science and Engineering: A*, 280(1):108–115, 2000.
- [22] Erol Feyzullahoğlu and Nehir Şakiroğlu. The wear of aluminium-based journal bearing materials under lubrication. *Materials & Design*, 31(5):2532–2539, 2010.
- [23] Robert L Greene, Warren J Whitney, and James M Carpenter. Lead-free bearing, 2004. US Patent 6,746,154.
- [24] Toshiaki Kawachi, Satoshi Takayanagi, Hiroyuki Asakura, and Hideo Ishikawa. Development of lead free overlay for three layer bearings of highly loaded engines. Technical report, SAE Technical Paper, 2005.
- [25] Florian Grün, István Gódor, Walter Gärtner, and Wilfried Eichlseder. Tribological performance of thin overlays for journal bearings. *Tribology International*, 44(11):1271–1280, 2011.
- [26] Toshiyuki Chitose, Shu Kamiya, Yasunori Kabeya, and Toru Desaki. Friction and wear reduction of engine bearings with solid lubricant overlay. Technical report, SAE Technical Paper, 2014.

- [27] Friedrich Harig and Dominique Petit. Polyfluorocarbon coated metal bearing, November 12 1996. US Patent 5,573,846.
- [28] Jan Lundberg. Influence of surface roughness on normal-sliding lubrication. *Tribology international*, 28(5):317–322, 1995.
- [29] Li Xiao, B-G Rosen, Naser Amini, and Per H Nilsson. A study on the effect of surface topography on rough friction in roller contact. *Wear*, 254(11):1162–1169, 2003.
- [30] Ramesh Singh, Shreyes N Melkote, and Fukuo Hashimoto. Frictional response of precision finished surfaces in pure sliding. *Wear*, 258(10):1500–1509, 2005.
- [31] Florian Summer, Florian Grün, Jürgen Schiffer, István Gódor, and Ilias Papadimitriou. Tribological study of crankshaft bearing systems: Comparison of forged steel and cast iron counterparts under start-stop operation. *Wear*, 338:232–241, 2015.
- [32] Riaz A Mufti and Martin Priest. Experimental evaluation of piston-assembly friction under motored and fired conditions in a gasoline engine. *Journal of tribology*, 127(4):826–836, 2005.
- [33] Akihiro Kose, Motohiko Koushima, Tomohiro Ukai, Yuki Kawashima, and Kouji Zushi. Development of lead-free al-sn-si alloy bearing for recent automotive engines. Technical report, SAE Technical Paper, 2014.

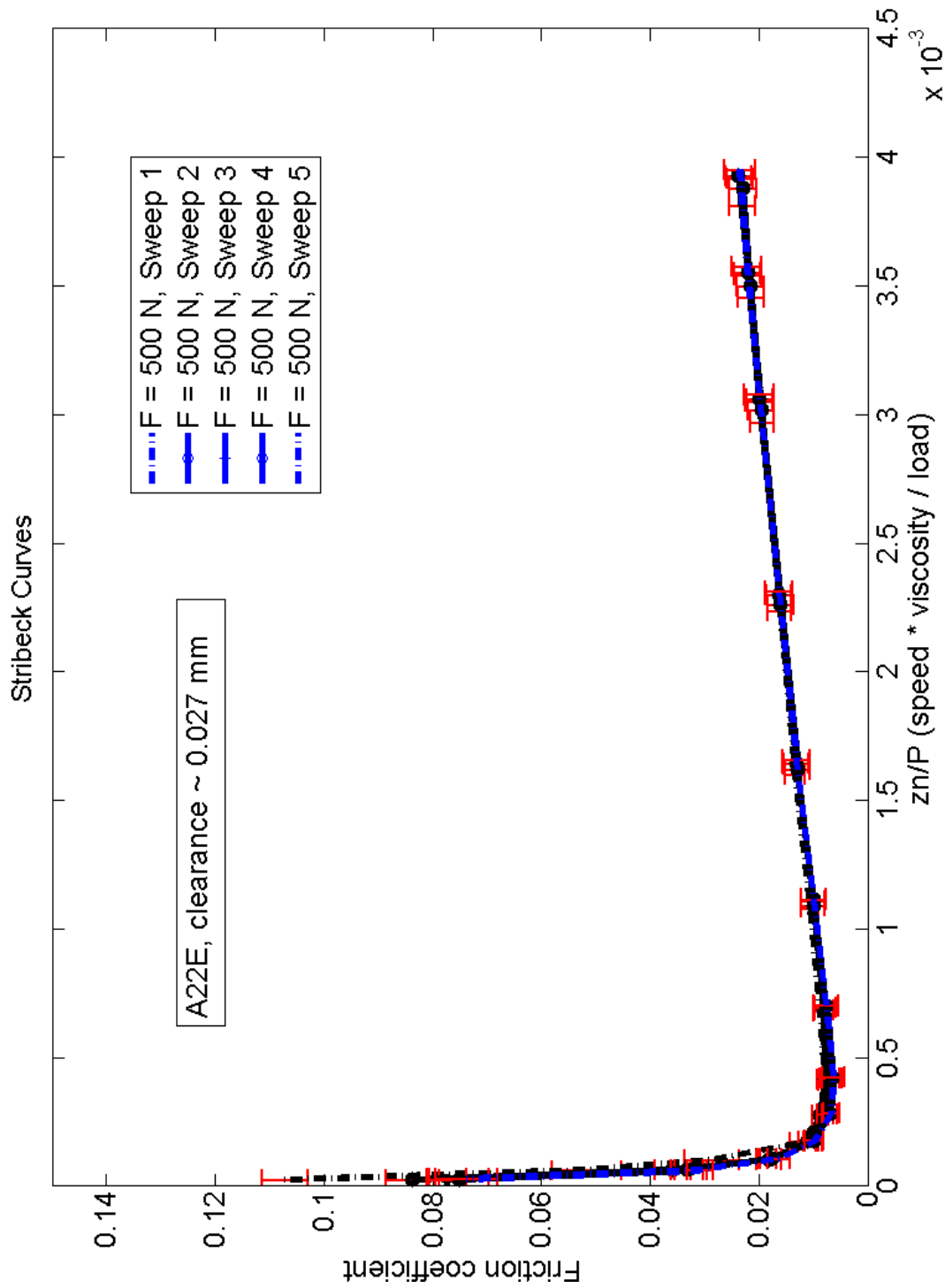
Appendix



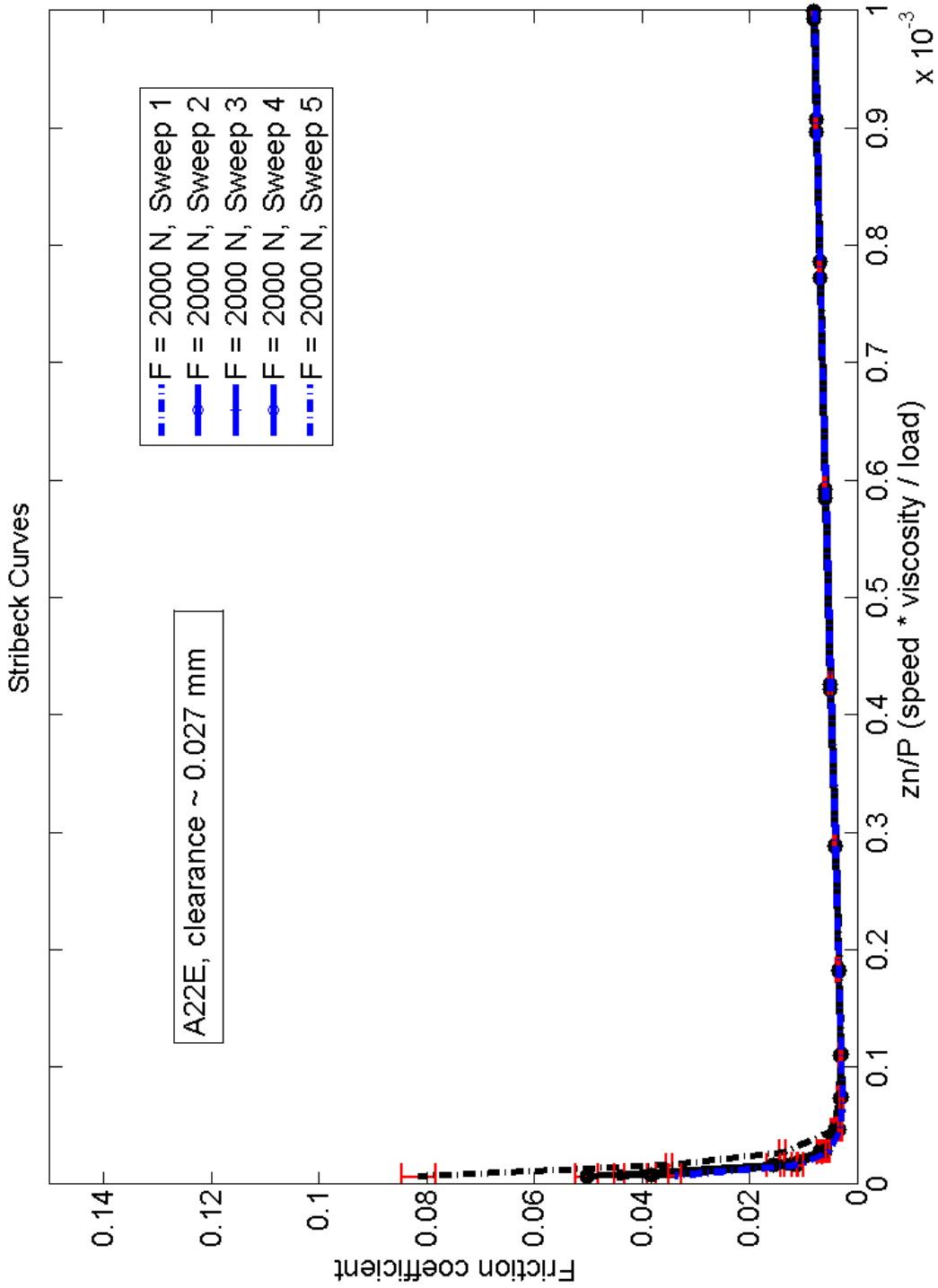
A1: Strubeck diagram, representing the frictional performance of the A22E bearing material under reduced load, at 500 N. Values for coefficient of friction. HL regime: 0.025 with $\sigma = 0.003$ at start, 0.026 with $\sigma = 0.002$ at end. BL regime: 0.107 with $\sigma = 0.010$ at start, 0.061 with $\sigma = 0.006$ at end. Minimum value: 0.007 with $\sigma = 0.002$.



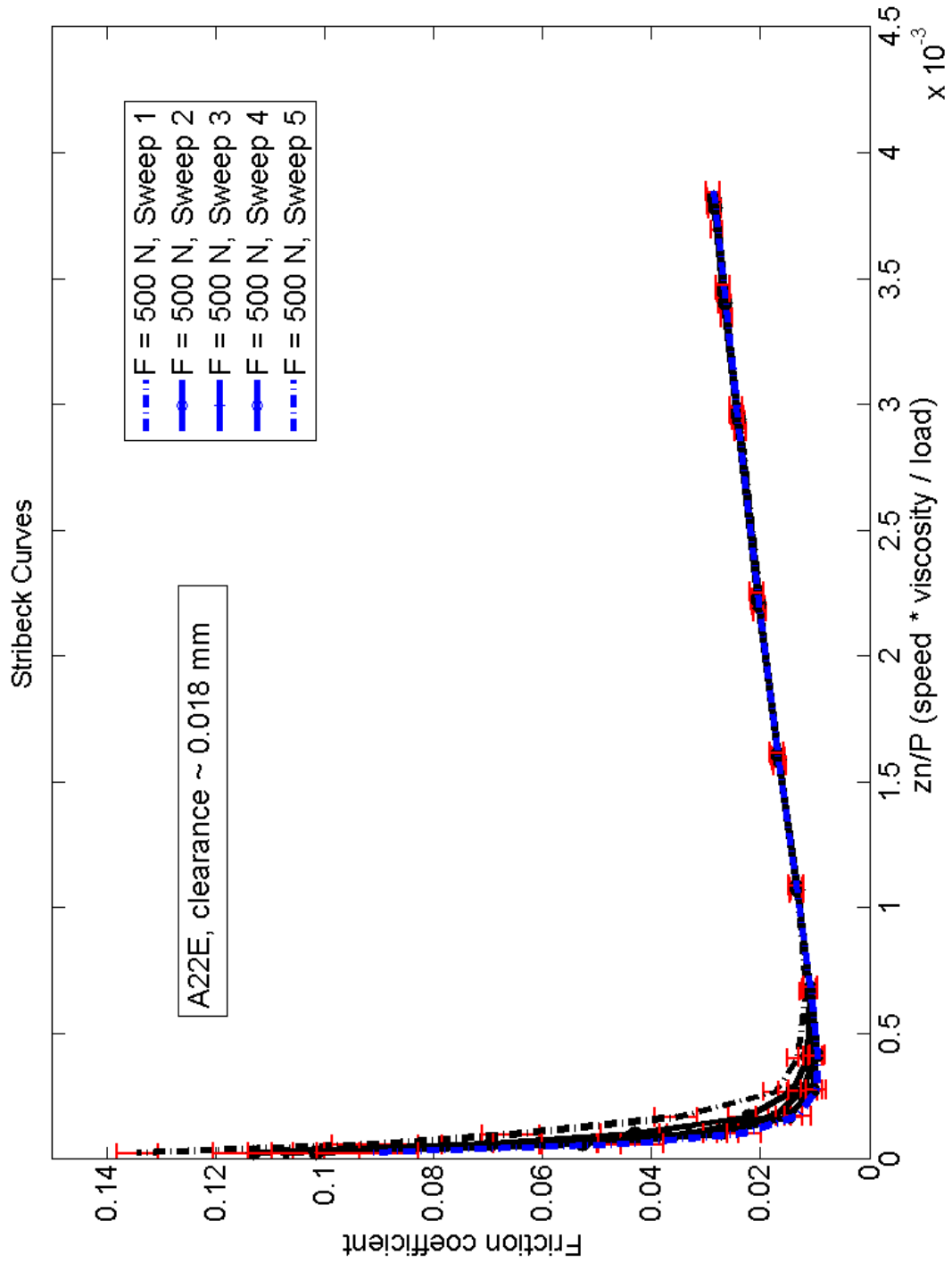
A2: Stribeck diagram, representing the frictional performance of the A22E bearing material under full load, at 2000 N. Values for coefficient of friction. HL regime: 0.008 with $\sigma = 0.001$ at start, 0.008 with $\sigma = 0.001$ at end. BL regime: 0.081 with $\sigma = 0.001$ at start, 0.048 with $\sigma = 0.0008$ at end. Minimum value: 0.003 with $\sigma = 0.001$.



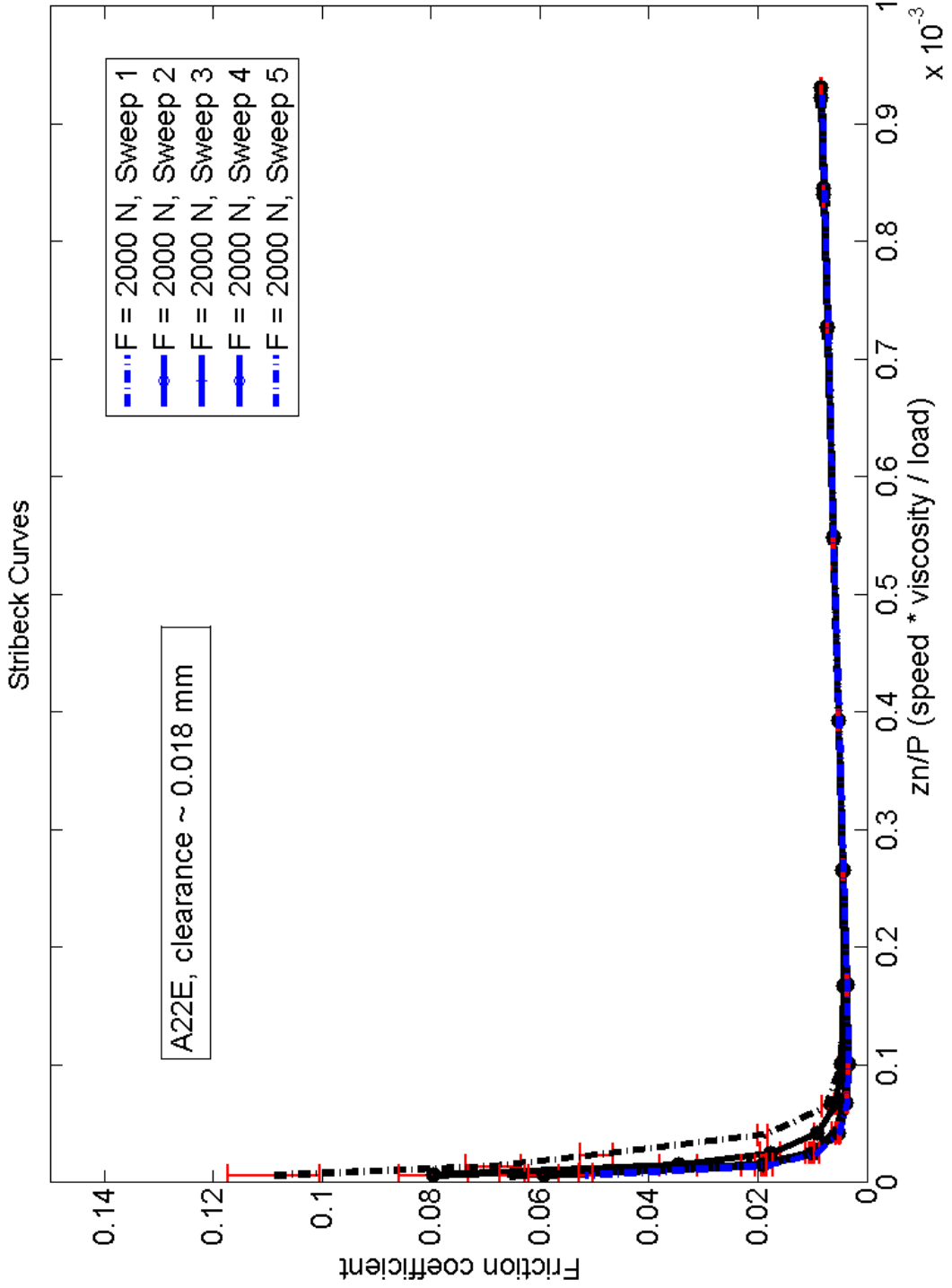
A3: Stribeck diagram, representing the frictional performance of the A22E bearing material under reduced load, at 500 N. Values for coefficient of friction. HI regime: 0.022 $\sigma = 0.002$ at start, 0.023 with $\sigma = 0.002$ at end. BL regime: 0.107 with $\sigma = 0.004$ at start, 0.073 with $\sigma = 0.005$ at end. Minimum value: 0.006 with $\sigma = 0.002$.



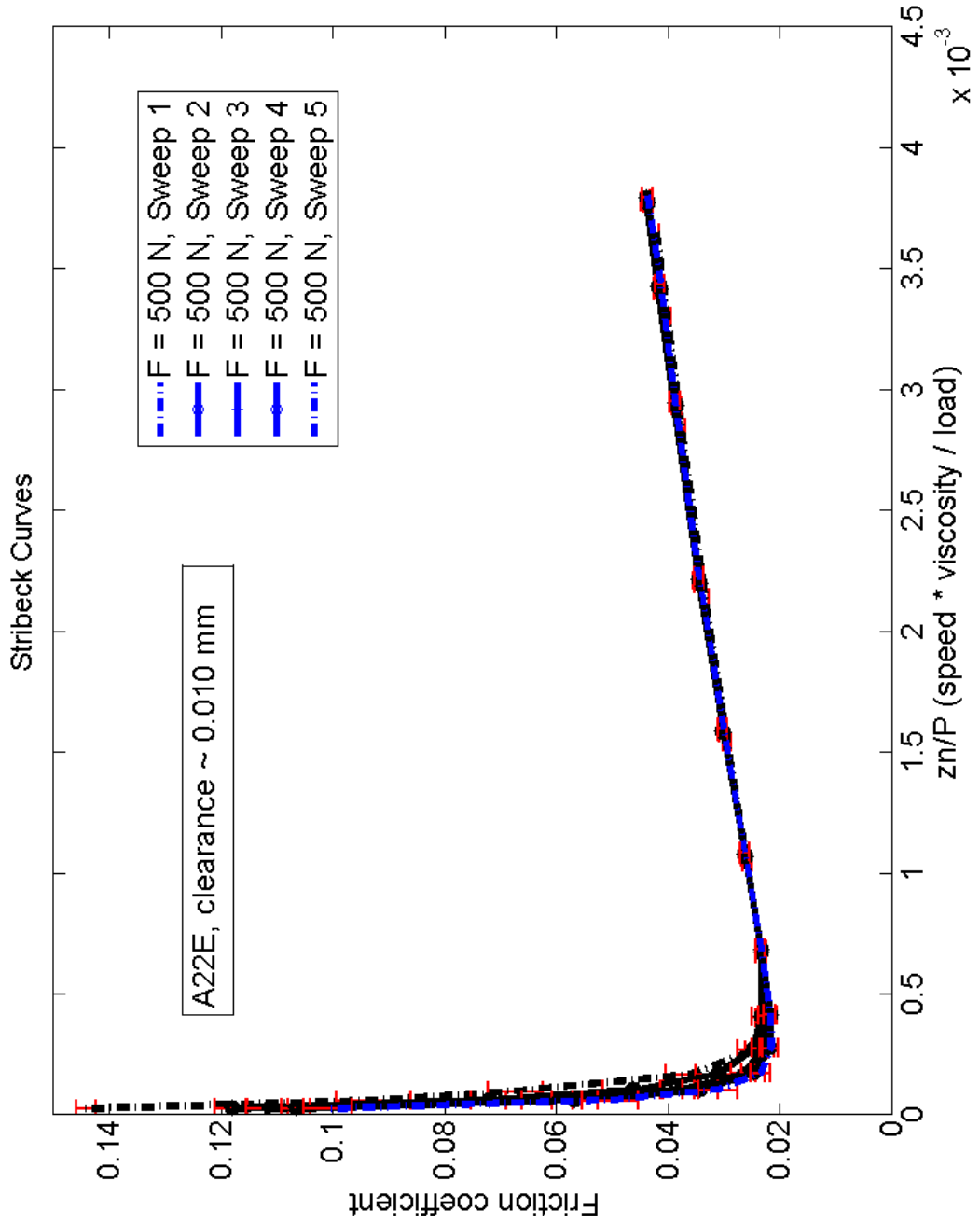
A4: Strubeck diagram, representing the frictional performance of the A22E bearing material under full load, at 2000 N. Values for coefficient of friction. HI regime: 0.007 $\sigma = 0.0002$ at start, 0.007 with $\sigma = 0.0002$ at end. BL regime: 0.081 with $\sigma = 0.003$ at start, 0.033 with $\sigma = 0.0012$ at end. Minimum value: 0.002 with $\sigma = 0.0003$.



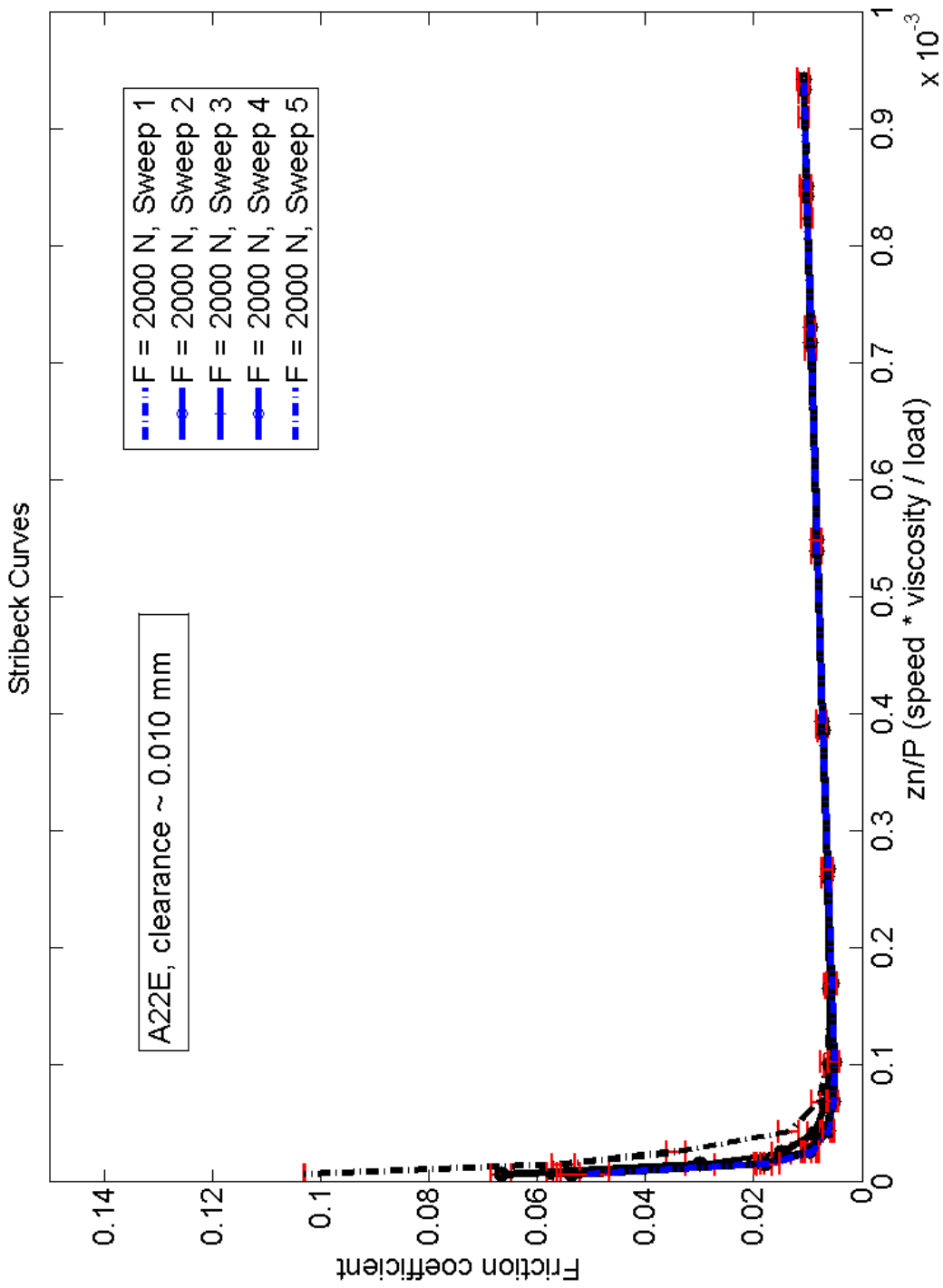
A5: Stribeck diagram, representing the frictional performance of the A22E bearing material under reduced load, at 500 N. Values for coefficient of friction. HI regime: 0.027 $\sigma = 0.001$ at start, 0.028 with $\sigma = 0.0012$ at end. BL regime: 0.134 with $\sigma = 0.0038$ at start, 0.092 with $\sigma = 0.0092$ at end. Minimum value: 0.009 with $\sigma = 0.0014$.



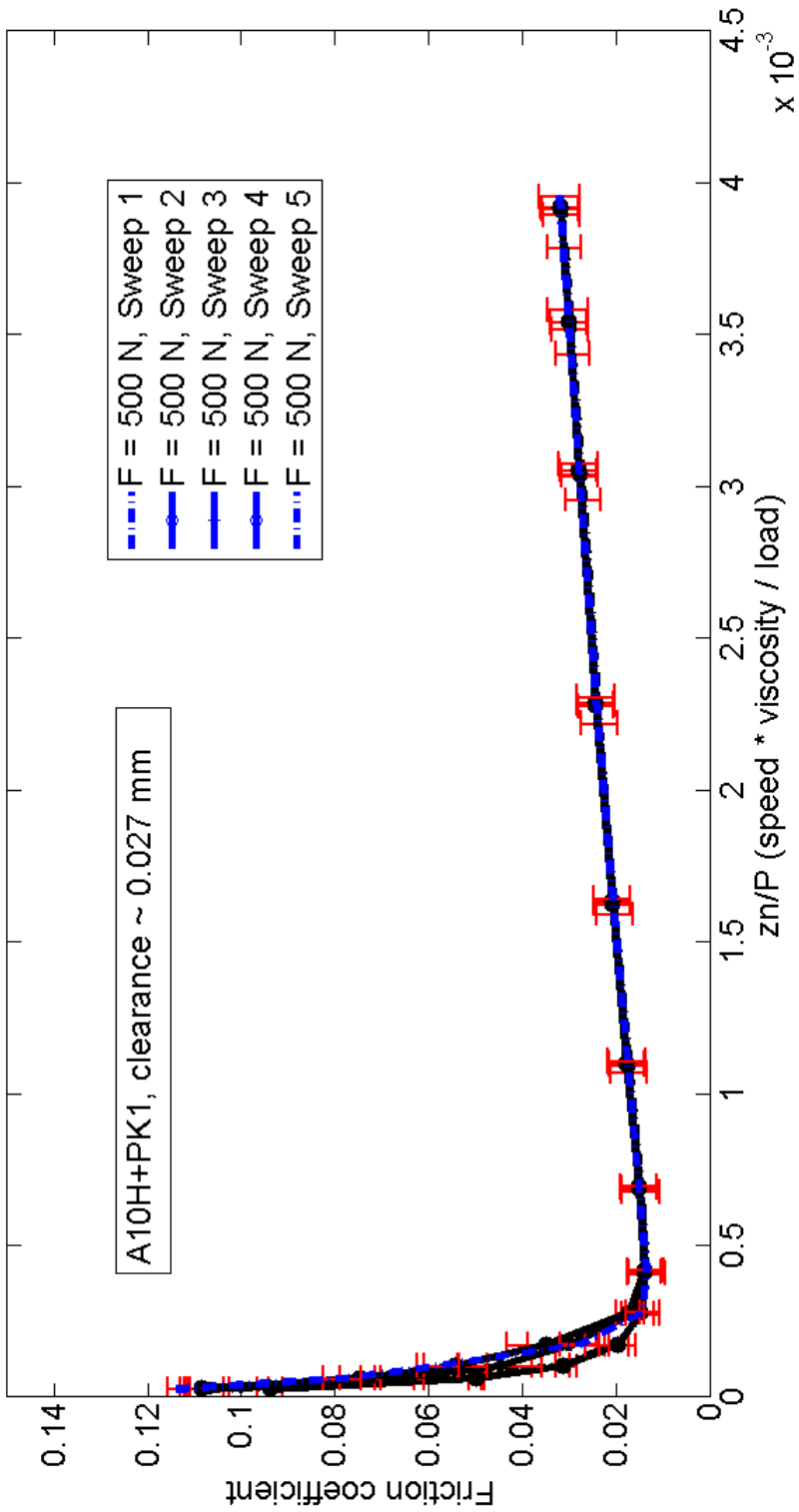
A6: Stribeck diagram, representing the frictional performance of the A22E bearing material under full load, at 2000 N.
 Values for coefficient of friction. HI regime: $\sigma = \text{at start}$, with $\sigma = \text{at end}$. BL regime: with $\sigma = \text{at start}$, with $\sigma = \text{at end}$. Minimum value: with $\sigma = \text{at end}$.



A7: Stribeck diagram, representing the frictional performance of the A22E bearing material under reduced load, at 500 N.
 Values for coefficient of friction. HL regime: 0.042 $\sigma = 0.0005$ at start, 0.043 with $\sigma = 0.0009$ at end. BL regime: 0.144 with $\sigma = 0.001$ at start, 0.100 with $\sigma = 0.004$ at end. Minimum value: 0.021 with $\sigma = 0.001$.

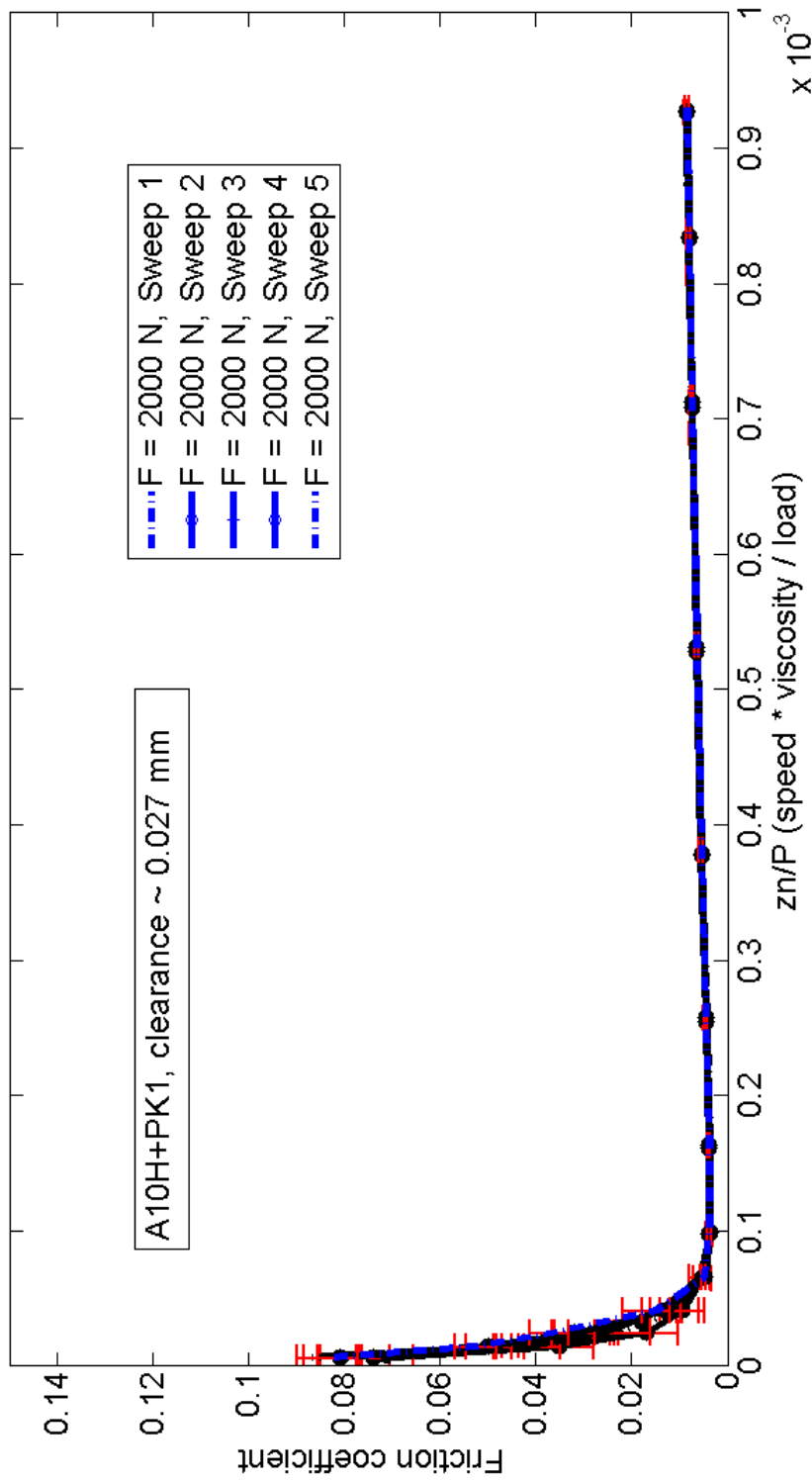


A8: Strubeck diagram, representing the frictional performance of the A22E bearing material under full load, at 2000 N. Values for coefficient of friction. HI regime: 0.010 $\sigma = 0.001$ at start, 0.010 with $\sigma = 0.0009$ at end. BL regime: 0.103 with $\sigma = 0.0001$ at start, 0.051 with $\sigma = 0.0047$ at end. Minimum value: 0.005 with $\sigma = 0.0009$.



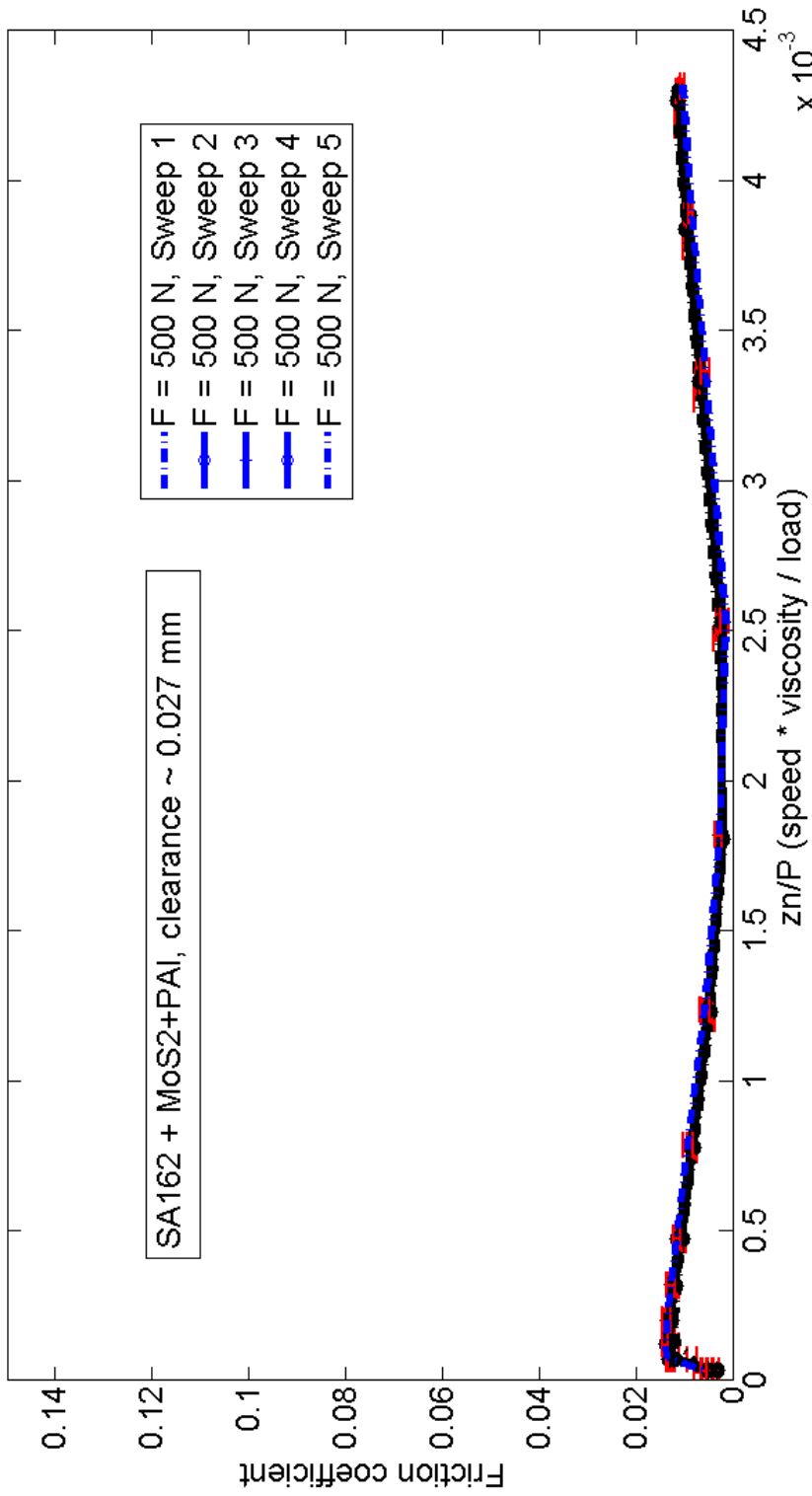
A9: Striebeck diagram, representing the frictional performance of the A10H bearing material coated with PK1 overlay, under reduced load, at 500 N.

Values for coefficient of friction. HL regime: 0.030 $\sigma = 0.003$ at start, 0.032 with $\sigma = 0.004$ at end. BL regime: 0.102 with $\sigma = 0.008$ at start, 0.113 with $\sigma = 0.001$ at end. Minimum value: 0.013 with $\sigma = 0.004$.

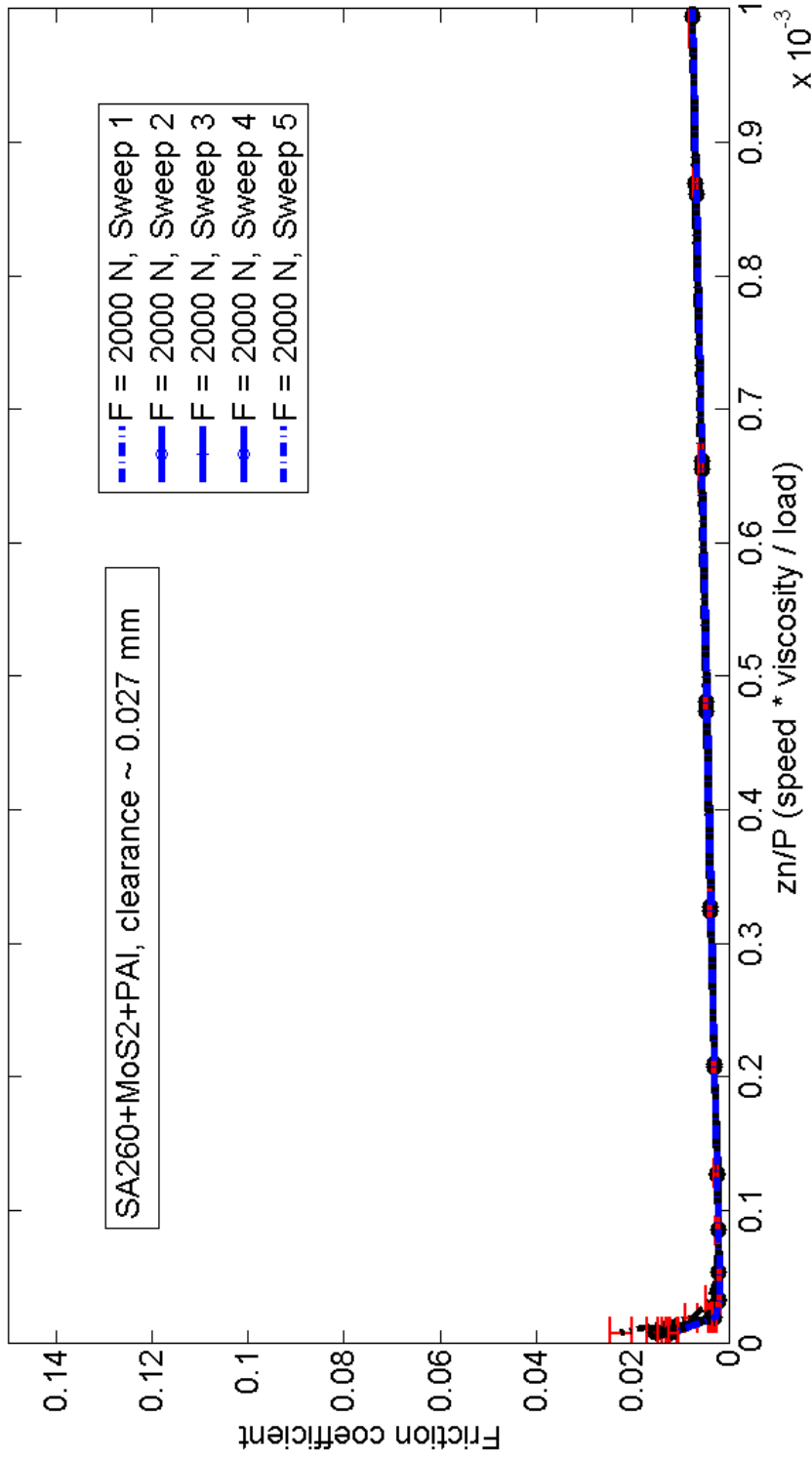


A10: Stribeck diagram, representing the frictional performance of the A10H bearing material coated with PK1 overlay under full load, at 2000 N.

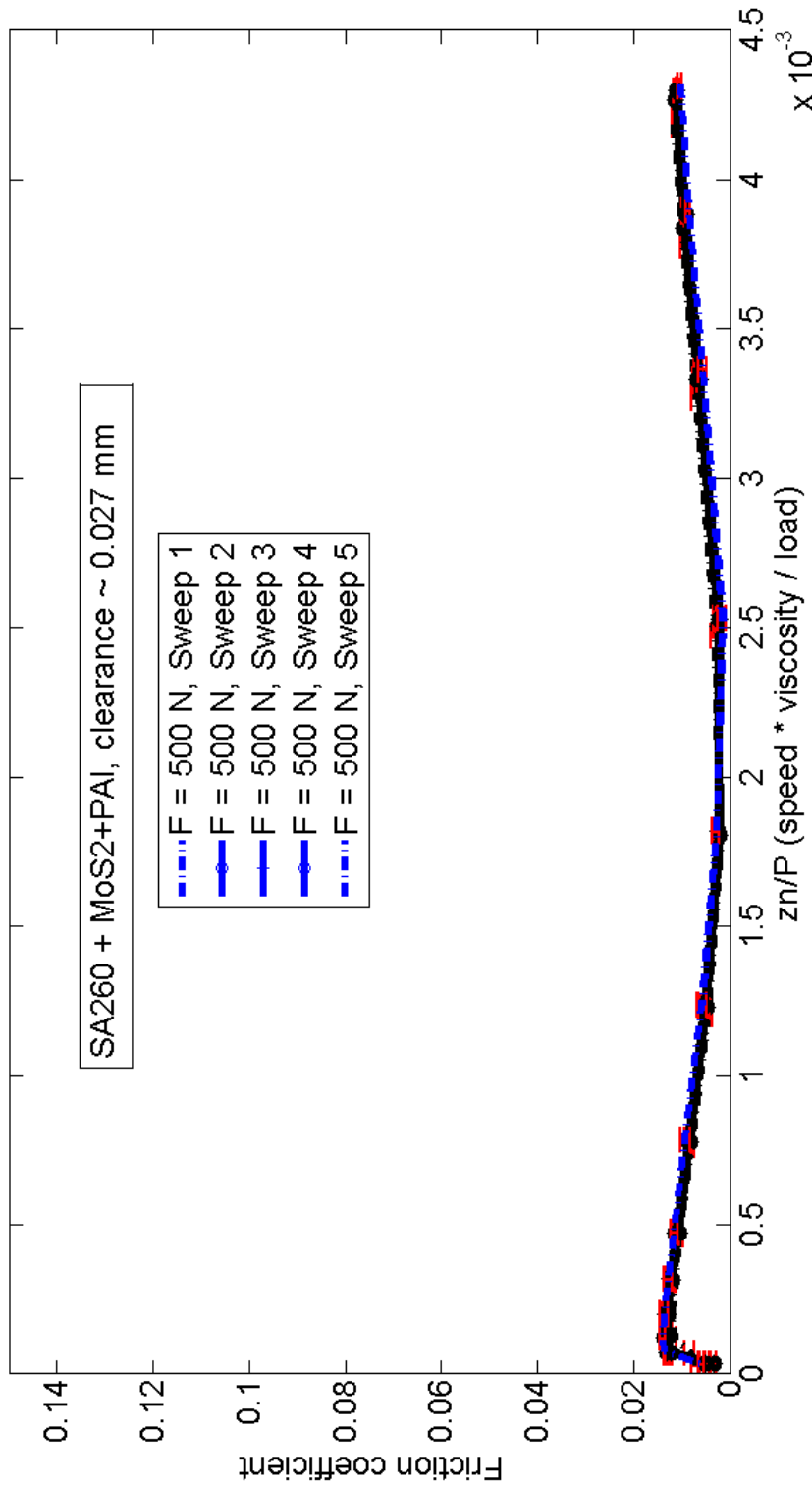
Values for coefficient of friction. HL regime: 0.008 $\sigma = 0.0004$ at start, 0.008 with $\sigma = 0.0003$ at end. BL regime: 0.087 with $\sigma = 0.002$ at start, 0.082 with $\sigma = 0.005$ at end. Minimum value: 0.003 with $\sigma = 0.0004$.



A11: Stribeck diagram, representing the frictional performance of the bearing material coated with MoS₂+PAI overlay, under reduced load, at 500 N. Lubricant OW-20.
 Values for coefficient of friction. HI regime: 0.011 $\sigma = 0.0004$ at start, 0.01 with $\sigma = 0.0003$ at end. BL regime: 0.007 with $\sigma = 0.0007$ at start, 0.006 with $\sigma = 0.0004$ at end. Minimum value: 0.001 with $\sigma = 0.0008$.

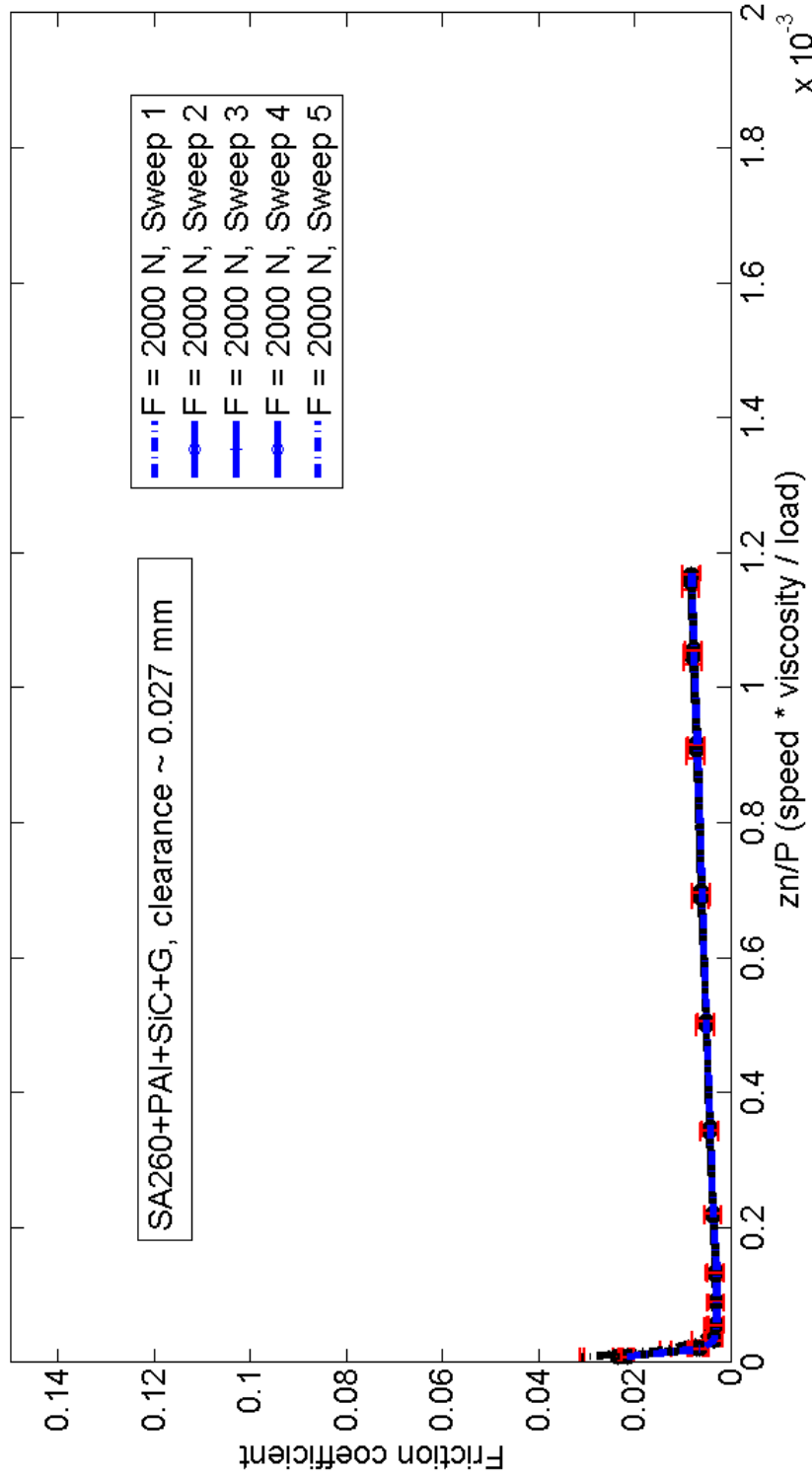


A12: Stribeck diagram, representing the frictional performance of the bearing material coated with MoS₂+PAI overlay, under full load, at 2000 N.
 Values for coefficient of friction. HL regime: 0.0081 $\sigma = 0.0003$ at start, 0.008 with $\sigma = 0.0003$ at end. BL regime: 0.022 with $\sigma = 0.0022$ at start, 0.011 with $\sigma = 0.0009$ at end. Minimum value: 0.001 with $\sigma = 0.0003$.

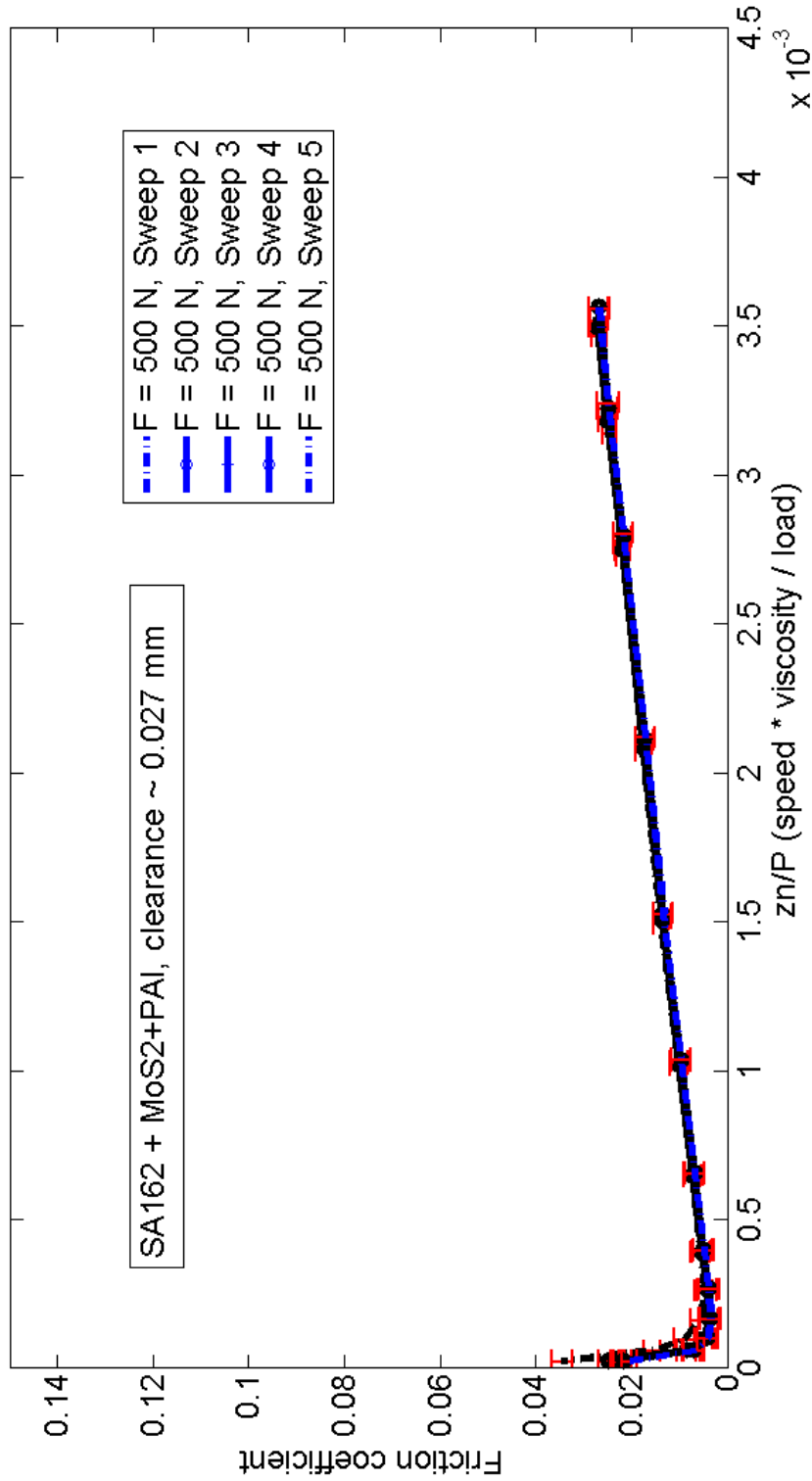


A13: Trail 1.1.3. Stribeck diagram, representing the frictional performance of the bearing material coated with PAI+SiC+graphite overlay, under reduced load, at 500 N.

Values for coefficient of friction. HI regime: 0.028 $\sigma = 0.001$ at start, 0.028 with $\sigma = 0.002$ at end. BL regime: 0.028 with $\sigma = 0.002$ at start, 0.02 with $\sigma = 0.002$ at end. Minimum value: 0.005 with $\sigma = 0.001$.

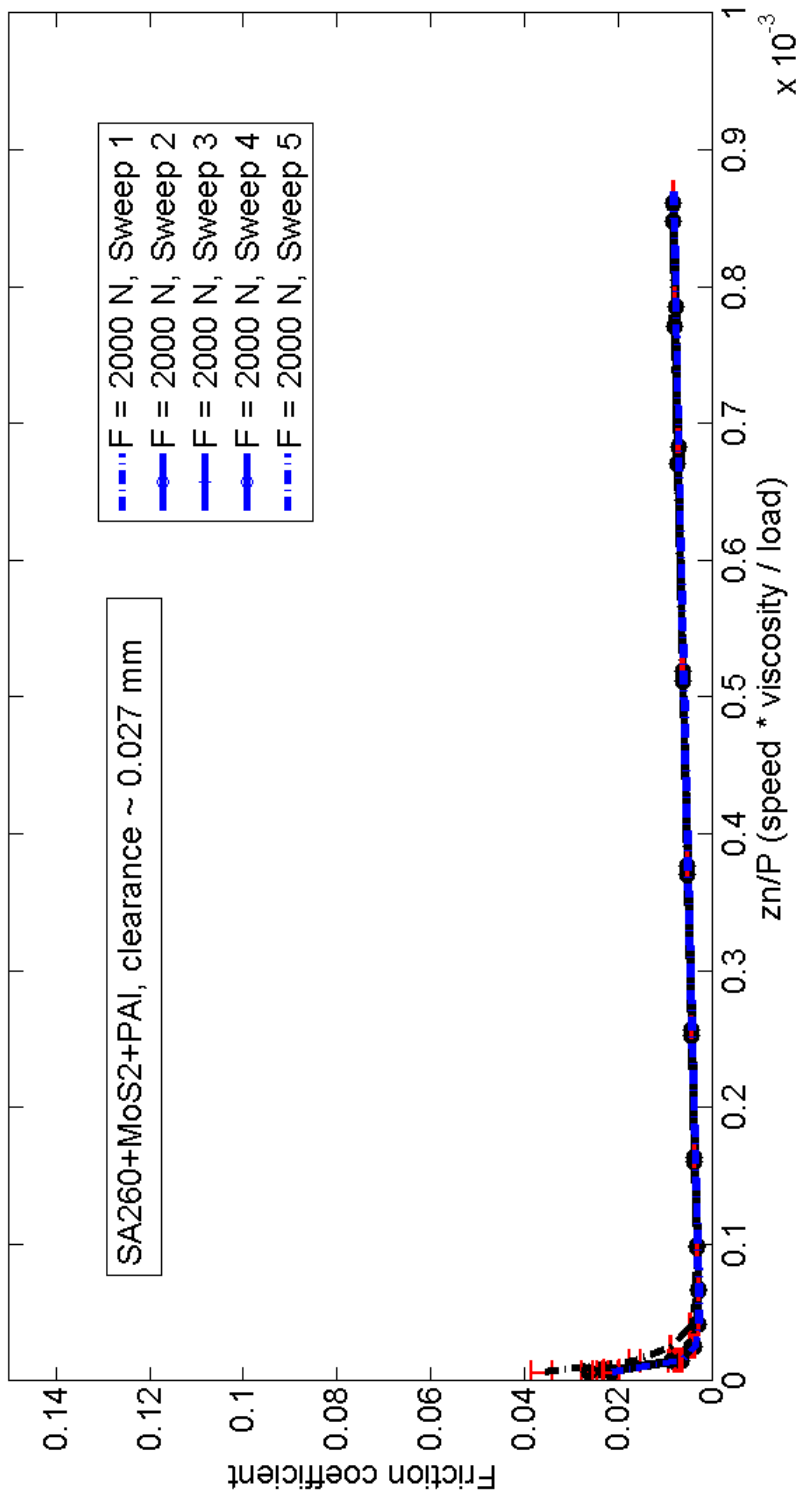


A14: Trail 2.1.3. Stribeck diagram, representing the frictional performance of the bearing material coated with PAI+SiC+graphite overlay, under full load, at 2000 N.
 Values for coefficient of friction. HL regime: 0.008 $\sigma = 0.001$ at start, 0.008 with $\sigma = 0.001$ at end. BL regime: 0.03 with $\sigma = 0.0004$ at start, 0.021 with $\sigma = 0.001$ at end. Minimum value: 0.002 with $\sigma = 0.001..$



A15: Stribeck diagram, representing the frictional performance of the bearing material coated with MoS₂+PAI overlay, under reduced load, at 500 N. Lubricant OW-16.

Values for coefficient of friction. HL regime: 0.026 $\sigma = 0.001$ at start, 0.026 with $\sigma = 0.002$ at end. BL regime: 0.034 with $\sigma = 0.002$ at start, 0.020 with $\sigma = 0.001$ at end. Minimum value: 0.003 with $\sigma = 0.002$.



A16: Stribeck diagram, representing the frictional performance of the bearing material coated with MoS₂+PAI overlay, under full load, at 2000 N. Lubricant OW-16.
 Values for coefficient of friction. HL regime: 0.008 $\sigma = 0.0002$ at start, 0.008 with $\sigma = 0.0001$ at end. BL regime: 0.036 with $\sigma = 0.002$ at start, 0.021 with $\sigma = 0.001$ at end. Minimum value: 0.002 with $\sigma = 0.0001$.